



1 **Estimates of critical loads and exceedances of acidity and**  
2 **nutrient nitrogen for mineral soils in Canada for 2014–2016**  
3 **average annual sulphur and nitrogen atmospheric deposition**

4  
5 Hazel Cathcart<sup>1</sup>, Julian Aherne<sup>2</sup>, Michael D. Moran<sup>1\*</sup>, Verica Savic-Jovicic<sup>1</sup>, Paul A. Makar<sup>1</sup>, and  
6 Amanda Cole<sup>1</sup>.

7 <sup>1</sup>Air Quality Research Division, Atmospheric Science and Technology Directorate, Science and Technology Branch,  
8 Environment and Climate Change Canada, Toronto, Ontario, M3H 5T4, Canada

9 <sup>2</sup>School of the Environment, Trent University, Peterborough, Ontario, K9L 0G2, Canada

10 \*Scientist emeritus

11

12 *Correspondence to:* Hazel Cathcart (hazel.cathcart@ec.gc.ca)

13 **Abstract.** The steady-state Simple Mass Balance model was applied to natural and semi-natural terrestrial  
14 ecosystems across Canada to produce nation-wide critical loads of acidity (maximum sulphur,  $CL_{maxS}$ ; maximum  
15 nitrogen,  $CL_{maxN}$ ; minimum nitrogen,  $CL_{minN}$ ) and nutrient nitrogen ( $CL_{nutN}$ ) at 250 m resolution. Parameterization  
16 of the model for Canadian ecosystems was considered with attention to the selection of the chemical criterion for  
17 damage at a site-specific resolution, with comparison between protection levels of 5% and 20% growth reduction  
18 (approximating commonly chosen base-cation-to-aluminum ratios of 1 and 10 respectively). Other parameters  
19 explored include modelled base cation deposition and site-specific nutrient and base cation uptake estimates based  
20 on North American tree chemistry data and tree species and biomass maps. Soil critical loads of nutrient nitrogen  
21 were also mapped using the Simple Mass Balance model. Critical loads of acidity were estimated to be low (e.g.,  
22 below  $500 \text{ eq}^{-1} \text{ ha yr}^{-1}$ ) for much of the country, particularly above  $60^\circ\text{N}$  latitude where base cation weathering rates  
23 are low due to cold annual average temperature. Exceedances were mapped relative to annual sulphur and nitrogen  
24 deposition averaged over 2014–2016. Results show that under a conservative estimate (5% protection level), 10%  
25 of Canada's Protected and Conserved Areas in the study area experienced exceedance of some level of soil critical  
26 load of acidity while 70% experienced exceedance of soil critical load of nutrient nitrogen.

27 **1 Introduction**

28 During the last three decades, reductions in sulphur (S) and nitrogen (N) emissions and acidic deposition have led to  
29 improvements in ecosystem health across the U.S. and Canada; nonetheless, the acid rain question remains relevant  
30 in Canada. Large point sources of emissions in western Canada have emerged, prompting concerns of impacts to  
31 sensitive ecosystems in British Columbia and the Athabasca Oil Sands Region (AOSR) in northeastern Alberta (e.g.,  
32 Mongeon et al., 2010; Williston et al., 2016; Makar et al., 2018). Further, increased marine traffic in the Arctic due  
33 to the effects of anthropogenic warming has raised questions about potential impacts of acidic deposition on  
34 northern ecosystems already under pressure from climate change (Forsius et al., 2010; Liang and Aherne, 2019).  
35 Recovery of forest soils from decades of elevated acidic deposition in the northeastern U.S. and eastern Canada is



36 encouraging, but is predicted to be slow (Lawrence et al., 2015; Hazlett et al., 2020) and is complicated by the effect  
37 of elevated N deposition (Clark et al., 2013; Simkin et al., 2016; Pardo et al., 2019; Wilkins et al., 2023) and climate  
38 change (Wu and Driscoll, 2010). The importance of N deposition to acidification and eutrophication has received  
39 increased recognition in recent years, prompting new avenues of risk assessment and mapping (e.g. empirical critical  
40 loads of nitrogen; (Bobbink et al., 2022; Bobbink and Hicks, 2014). While N oxide emissions in Canada declined  
41 by 41% between 1990 and 2022, ammonia emissions increased by 24% in that same period (ECCC, 2024).

42

43 The critical loads concept, defined as “the maximum deposition that will not cause chemical changes leading to  
44 long-term harmful effects on ecosystem structure and function” (Nilsson and Grenfelt, 1988) is the primary tool for  
45 identifying ecosystems that are sensitive to air pollution, particularly with respect to acidification and eutrophication  
46 (De Vries et al., 2015; Burns et al., 2008). Ecosystems that receive acidic deposition above their critical load are  
47 said to be in exceedance; that is, they are at risk of undergoing biological damage. Soil acidification is characterized  
48 by attrition of base cations and a decrease in soil pH, which in turn causes leaching of toxic metals, such as  
49 aluminum, and damage to plant roots. During the past three decades, these effects have been observed in forest soils  
50 in the northeastern U.S. and eastern Canada (e.g., Cronan and Schofield, 1990; Likens et al., 1996; Lawrence et al.,  
51 1999) that received acidic deposition in excess of their critical loads. The effects of nutrient N on ecosystems,  
52 which include eutrophication, reduced plant biodiversity, and plant community changes, have also become an  
53 emerging issue, with studies suggesting that some Canadian ecosystems are in exceedance of their nutrient N critical  
54 load (e.g., Aherne and Posch, 2013; Reinds et al., 2015; Williston et al., 2016).

55

56 The standard approach for estimating soil critical loads is the Simple Mass Balance (SMB) model (Sverdrup and De  
57 Vries, 1994, Posch et al., 2015), a steady-state model with several simplifying assumptions to reduce input  
58 requirements. This approach has been used for regional and provincial critical load assessments in Canada (e.g.,  
59 Ouimet et al., 2006; Aklilu et al., 2022) as well as on a multi-provincial (NEG-ECP, 2001; Carou et al., 2008;  
60 Aherne and Posch, 2013) and national scale (Reinds et al., 2015). However, nationwide implementations of the  
61 SMB model in Canada have been challenged by data paucity and disharmony across provinces (i.e. different data  
62 sources, methodology and spatial alignment), coarse input map resolution, and computational difficulties driven by  
63 the size of the country and the subsequent size of data files used in critical load calculations. In recent years,  
64 though, high-resolution input data (for soils, meteorology, and forest composition) have become available and  
65 present an opportunity to refine, expand, and harmonise critical loads across the entire country, including extending  
66 maps into the Canadian Arctic. These developments come at a time when policymakers in Canada are seeking to  
67 define and track air quality impacts (such as those by acidic S and N deposition) on sensitive ecosystems under the  
68 Addressing Air Pollution Horizontal Initiative (ECCC, 2021). Furthermore, development of high-resolution critical  
69 loads of nutrient N to assess terrestrial eutrophication risk may contribute to efforts to meet biodiversity goals such  
70 as those under the Kunming-Montreal Global Biodiversity Framework (ECCC, 2023c). While the SMB model is a  
71 well-established and widely used approach to determine critical loads, there remains a need for harmonised



72 application across Canadian ecosystems to provide maps from which the effect of S and N deposition can be  
73 estimated.

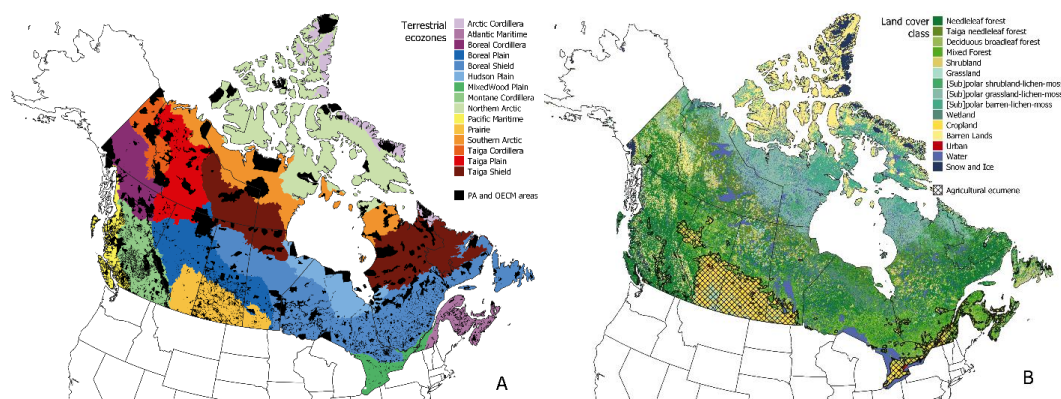
74

75 The objective of this study was to assess the impacts of acidic and nutrient N deposition on terrestrial ecosystems  
76 Canada-wide using the critical loads framework. In doing so, we applied a harmonised methodology to the SMB  
77 model for Canadian ecosystems using high-resolution input maps, including modelled Canada-wide base cation  
78 deposition (crucial for the estimation of critical loads). We also explored the choice of chemical (damage) criterion  
79 for Canadian ecosystems using a site-specific approach. Finally, we assessed the impact of anthropogenic base  
80 cation deposition on exceedance estimates under annual average S and N deposition (ECCC, 2023a) for the three-  
81 year period 2014–2016, using the Canadian Protected and Conserved Areas Database (CPCAD; ECCC, 2023b), to  
82 evaluate risk to sites that may be of interest to policymakers.

## 83 **2 Methods**

### 84 **2.1 Study area**

85 As the second-largest country by landmass in the world at over 9.9 million km<sup>2</sup>, Canada is home to a variety of  
86 climates, soils, vegetation, and geological structures that are often grouped into distinct ecozones (Figure 1A). The  
87 full extent of Canada was included in this study to bring together estimates for all 10 provinces and 3 territories.  
88 However, only natural and semi-natural soils meeting certain criteria for critical load estimations were considered.  
89 A land cover map (CEC, 2018) was used to exclude non-soil ecosystems including water, wetlands, and permanent  
90 snow and ice (see Figure 1B). Soils were further limited to natural and semi-natural ecosystems by excluding urban  
91 areas, crop classes, and areas within the boundaries of the agricultural ecumene (Figure 1B). Areas considered  
92 “barren” by land classification were not excluded when soil depth was indicated. Since peat and wetland soil  
93 classification is difficult at a Canada-wide scale (i.e. data at the required scale are presently unavailable), organic  
94 soils with 30% or more organic matter content were filtered out. The Hudson Plain ecozone (which contains the  
95 world’s largest contiguous wetland) was also broadly excluded from the study because of very low mineral soil  
96 coverage.

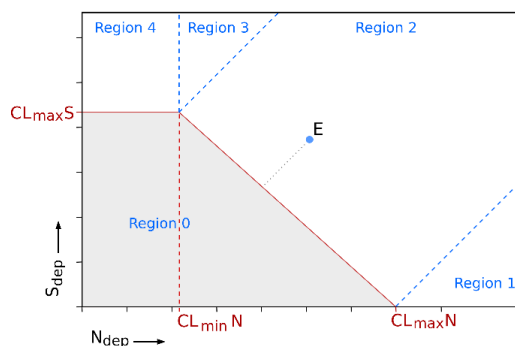


97 **Figure 1: Study area illustrating the 15 terrestrial ecozones of Canada (A, data source: Agriculture and Agri-Food**  
 98 **Canada, 2013) with terrestrial Protected and Other Effective area-based Conservation Measures (OECD areas in black**  
 99 **(ECCC, 2023b), as well as 15 land cover classes (B, data source: CEC, 2018) with agricultural regions in crosshatch**  
 100 **(Statistics Canada, 2017).**

101

102 **2.2 The Simple Mass Balance model for acidity and nutrient nitrogen**

103 Critical loads of acidity were estimated using the SMB model, which balances sources, sinks, and outflows of S and  
 104 N in terrestrial ecosystems while assuming ecosystems are at long-term equilibrium (i.e. about 100 years,  
 105 representing at least one forest rotation cycle) (CLRTAP, 2015). The SMB model defines the critical load of S and  
 106 N acidity (Figure 2) as a function of the maximum S critical load ( $CL_{maxS}$ ), the maximum N critical load ( $CL_{maxN}$ ),  
 107 and the amount of N taken up by the ecosystem ( $CL_{minN}$ ). Pairs of S and N deposition that fall outside this function  
 108 (white region, Figure 2) signify that the receiving ecosystem is in exceedance of its critical load of acidity (i.e., it  
 109 receives a potentially damaging amount of acidic deposition).



110

111 **Figure 2: The acidity critical load function (red line) is defined by the maximum sulphur critical load ( $CL_{maxS}$ ), the**  
 112 **maximum nitrogen critical load ( $CL_{maxN}$ ) and the minimum nitrogen critical load ( $CL_{minN}$ ). Deposition points falling**  
 113 **outside the critical load function (e.g., point E) are in exceedance (and defined as Regions 1-4), while those within the grey**  
 114 **area (Region 0) are protected.**



115 The determination of  $CL_{max}S$  requires knowledge of non-sea salt base cation (calcium, magnesium, potassium,  
 116 sodium) deposition ( $BC_{dep}$ ), soil base cation weathering ( $BC_{we}$ ), chloride deposition ( $Cl_{dep}$ ), base cation uptake  
 117 ( $Bc_{up}$ ), and the critical leaching of Acid Neutralizing Capacity (the ability of the ecosystem to buffer incoming  
 118 acidity), denoted  $ANC_{le,crit}$  (see Eq. 1). Note that sodium is included in some base cation terms (denoted BC, e.g.,  
 119  $BC_{we}$ ) when sodium contributes to buffering, but where it concerns uptake by vegetation sodium is omitted since it  
 120 is non-essential to plants (denoted Bc, e.g.,  $Bc_{up}$ ).

121

$$122 \quad CL_{max}S = BC_{dep} + BC_{we} - Cl_{dep} - Bc_{up} - ANC_{le,crit} \quad (1)$$

123

124 The value of  $ANC_{le,crit}$  (see Eq. (2)) is determined from a critical base-cation-to-aluminum ratio ( $Bc/Al_{crit}$ ), which is  
 125 set to protect the chosen biota within ecosystems of interest (i.e., the critical chemical criterion), soil percolation or  
 126 runoff (Q), and the gibbsite equilibrium constant ( $K_{gibb}$ ).

127

$$128 \quad ANC_{le,crit} = -Q^{\frac{2}{3}} \cdot \left( 1.5 \cdot \frac{BC_{dep} + BC_{we} - Bc_{up}}{K_{gibb} \cdot \left(\frac{Bc}{Al}\right)_{crit}} \right)^{\frac{1}{3}} - \left( 1.5 \cdot \frac{BC_{dep} + BC_{we} - Bc_{up}}{\left(\frac{Bc}{Al}\right)_{crit}} \right) \quad (2)$$

129

130 The calculation of  $CL_{min}N$  from Eq. (3) describes the limit above which N deposition becomes acidifying, where  $N_u$   
 131 denotes N taken up by vegetation and  $N_i$  denotes long-term net immobilization of N in the root zone of soils under  
 132 steady state conditions. A value of  $35.714 \text{ eq ha}^{-1} \text{ yr}^{-1}$  ( $0.5 \text{ kg N ha}^{-1} \text{ yr}^{-1}$ ) was used, based on estimates of annual  $N_i$   
 133 since the last glaciation by Rosen et al. (1992). Lastly,  $CL_{max}N$  is estimated from Eq. (4) using  $CL_{max}S$ ,  $CL_{min}N$ , and  
 134 the soil denitrification (the loss of nitrate to nitrogen gas) factor ( $f_{de}$ ).

135

$$136 \quad CL_{min}N = N_i + N_u \quad , \quad (3)$$

137

$$138 \quad CL_{max}N = CL_{min}N + \left( \frac{CL_{max}S}{1 - f_{de}} \right) \quad . \quad (4)$$

139

140 Equation (5) was used to estimate soil critical loads of nutrient N ( $CL_{nut}N$ ), wherein the acceptable inorganic N  
 141 leaching limit, a value set to prevent harmful effects of nutrient N such as eutrophication, vegetation community  
 142 changes, nutrient imbalances, and plant sensitivity to stressors, is set from acceptable N concentrations in soil  
 143 solution ( $[N]_{acc}$ ) multiplied by Q (CLRTAP 2015). The  $[N]_{acc}$  was set to  $0.0142 \text{ eq m}^{-3}$  ( $0.2 \text{ mg N l}^{-1}$  in soil solution)  
 144 for conifer forests and  $0.0214 \text{ eq m}^{-3}$  ( $0.3 \text{ mg N l}^{-1}$ ) for all other semi-natural vegetation, following the generalised  
 145 approach taken for the European critical loads database (Reinds et al., 2021) as values suggested in CLRTAP (2015)  
 146 are often country-specific and do not extend to other regions or ecosystems.

147

$$148 \quad CL_{nut}N = N_i + N_{up} + \left( \frac{Q \cdot [N]_{acc}}{1 - f_{de}} \right) \quad . \quad (5)$$



149 **2.3 Data and mapping**

150 Critical load estimates were calculated with the statistical programming language R, wherein inputs (Table 1) to and  
 151 outputs from the SMB model were represented by 250 m resolution raster maps. Alignment and projection in  
 152 WGS84 followed the layers sourced from the OpenLandMap.org project (i.e., Hengl (2018c, a, d, b); Hengl and  
 153 Wheeler (2018) in Table 1), since they represented the majority of input (raster) data sources. Output maps were  
 154 visualised using QGIS (QGIS Development Team, 2023) with accessible colour schemes (Tol, 2012). Acidity  
 155 critical load components ( $CL_{maxS}$ ,  $CL_{maxN}$ ,  $CL_{minN}$ ) and  $CL_{nutN}$  were all mapped using equivalents of acidity (or  
 156 nutrient nitrogen) per hectare per year ( $eq\ ha^{-1}\ yr^{-1}$ ).

157

158 **Table 1: Data sources for input parameters to the SMB model and critical load exceedance calculation.**

Parameter	Units	Use	Original resolution	Source
<b>Temperature</b>				
Average annual air temperature (1981–2010)	°C	BC <sub>we</sub>	250 m	McKenney et al., 2006
<b>Soil</b>				
Absolute depth to bedrock	cm	BC <sub>we</sub>	250 m	Hengl, 2017
Organic carbon	× 5 g kg <sup>-1</sup>	BC <sub>we</sub>	250 m	Hengl & Wheeler, 2018
Sand fraction	%	BC <sub>we</sub>	250 m	Hengl, 2018c
Clay fraction	%	BC <sub>we</sub>	250 m	Hengl, 2018a
Bulk density	g/cm <sup>3</sup>	BC <sub>we</sub>	250 m	Hengl, 2018d
Coarse fragment volume	%	BC <sub>we</sub>	250 m	Hengl, 2018b
Parent material acid class	class	BC <sub>we</sub>	250 m	CLBBR, 1996; SLCWG, 2010
Drainage class	class	BC <sub>we</sub>	250 m	CLBBR, 1996; SLCWG, 2010
Runoff (Q)	mm yr <sup>-1</sup>	ANC <sub>le,crit</sub>	0.05° x 0.1°	Reinds et al., 2015
<b>Vegetation</b>				
Tree species composition	%	B <sub>cup</sub> , N <sub>up</sub>	250 m	Beaudoin et al., 2014
Biomass	Mg ha <sup>-1</sup>			
Harvestable boundaries	km <sup>2</sup>	B <sub>cup</sub> , N <sub>up</sub>	250 m	Dymond et al., 2010
Tree chemistry database (U.S.)	% Ca, Mg, K, N	B <sub>cup</sub> , N <sub>up</sub>	-	Pardo et al., 2005
Tree chemistry database (Can.)	% Ca, Mg, K, N	B <sub>cup</sub> , N <sub>up</sub>	-	Paré et al., 2013
Land cover (2010)	class	Limiting extent	250 m	(CEC, 2018)
Agricultural ecumene (2016)	class	Limiting extent	5 km	Statistics Canada, 2017
Ecozones	class	Limiting extent, summary statistics	1:7.5 million	Agriculture and Agri-Food Canada, 2013
<b>Deposition</b>				
Base cation deposition (2010, 2016)	eq ha <sup>-1</sup> yr <sup>-1</sup>	ANC <sub>le,crit</sub>	12 km	(Galmarini et al., 2021)
Total mean S and N deposition	eq ha <sup>-1</sup> yr <sup>-1</sup>	Exceedance	10 km	(Moran et al., 2024b, a)



(2014–2016)

Canadian Protected and Conserved Areas Database	class	Identifying areas of special interest	Various	(ECCC, 2023b)
---	-------	---------------------------------------	---------	---------------

159

## 160 2.4 Base cation weathering

161 Generalised base cation weathering  $BC_{we}$  (i.e., calcium, magnesium, potassium and sodium) was mapped using the  
 162 soil type–texture approximation method, which assigns a base cation weathering class ( $BC_{w0}$ ) based on soil  
 163 characteristics (organic matter, sand, and clay percentage) and parent material acid class (see Eq. 6). Weathering is  
 164 modified by ambient temperature  $T$ , where  $A$  is the Arrhenius pre-exponential factor (3600 K), a temperature  
 165 coefficient for soil weathering (de Vries et al., 1992; CLRTAP, 2015). To address issues with resolution and  
 166 continuity across provinces, high-resolution (global 250 m) predicted soil maps from the OpenLandMap.org project  
 167 were used for the following input variables: bulk density ( $\rho$ ), organic carbon, coarse fragment volume (CF), and  
 168 sand and clay composition (see Table 1). One of the assumptions of the SMB model is that the soil compartment is  
 169 homogeneous; therefore, a weighted average for soil texture was developed based on layer depth, total depth ( $D$ ),  
 170 and corrections based on coarse fragment volume, percent organic matter, and bulk density. Percent organic matter  
 171 (OM) was obtained by dividing organic carbon (in  $\times 5 \text{ g kg}^{-1}$ ) by 2 (as recommended by Hengl & Wheeler, 2018;  
 172 Pribyl, 2010).

173

$$174 \quad BC_{we} = \left( \frac{\rho_{soil}}{\rho_{H_2O}} \right) D \left( 1 - \frac{CF}{100} \right) \left( 1 - \frac{OM}{100} \right) (BC_{w0} - 0.5) * 10^{\left( \frac{A}{281} - \frac{A}{273+T} \right)} \quad (6)$$

175

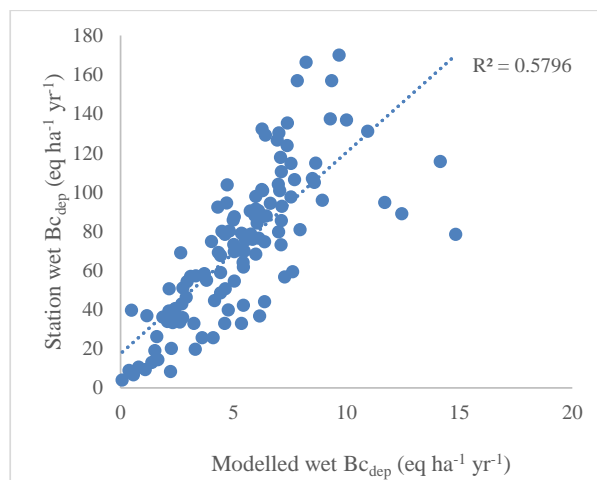
176 A second assumption is that the profile depth ( $D$ ) is limited to the root zone, which was set to a maximum of 50 cm  
 177 for forest soils and 30 cm for other land cover types such as shrubland, grassland and tundra. Soil depth was further  
 178 limited by an absolute-depth-to-bedrock global modelled map (Hengl, 2017; Shangquan et al., 2017) in case bedrock  
 179 was  $< 50$  cm. Base cation weathering omitting sodium ( $BC_{we}$ ) required for the calculation of  $ANC_{le,crit}$  (Eq. 2) was  
 180 scaled by 0.8 after CLRTAP (2015).

## 181 2.5 Base cation deposition

182 In the absence of modelled  $Bc_{dep}$  data, previous Canadian mapping studies have employed a single value, or coarsely  
 183 interpolated from limited Canadian Air and Precipitation Monitoring Network (CAPMoN) stations from 1994–1998  
 184 (Aklilu et al., 2022; Carou et al., 2008; Ouimet et al., 2006). Critical loads estimates for Canada by Reinds et al.  
 185 (2015) used coarse modelled global Ca deposition (Tegen and Fung, 1995) based on soil Ca content (Bouwman et  
 186 al., 2002) and estimated the other ions by regression. To address the gaps in data availability and spatial  
 187 distribution,  $Bc_{dep}$  in this study was sourced from modelled estimates produced with the Global Environmental  
 188 Multiscale–Modelling Air-quality and CHemistry (GEM-MACH) model at 12-km horizontal grid spacing for the air  
 189 quality multi-model comparison project AQMEII4 (Galmarini et al., 2021). Two different GEM-MACH



190 configurations, a version with detailed parameterizations and a second version with some simplified  
 191 parameterizations used for operational air-quality forecast simulations, estimated wet and dry non-sea-salt  $B_{c_{dep}}$  for  
 192 North America. Gridded annual deposition fields for two periods, 2010 and 2016, were obtained. Ideally, emissions  
 193 data sources used for S and N deposition and  $B_{c_{dep}}$  would be the same; however,  $B_{c_{dep}}$  is often not evaluated, and the  
 194 version of the emissions inventories used for S and N deposition did not include  $B_{c_{dep}}$ . Comparison of modelled wet  
 195  $B_{c_{dep}}$  to measured wet  $B_{c_{dep}}$  data from 33 Canadian Air and Precipitation Monitoring Network (CAPMoN)  
 196 precipitation-chemistry stations (Feng et al., 2021) and 87 U.S. National Atmospheric Deposition Monitoring  
 197 (NADP) precipitation-chemistry stations (NADP, 2023) within 300 km of the Canada-U.S. border showed that  
 198 modelled  $B_{c_{dep}}$  data were underestimated in each model configuration and year by an average factor of 15, though  
 199 the correlation was relatively high (Figure 3). A  $B_{c_{dep}}$  input map was prepared by averaging (wet plus dry)  $B_{c_{dep}}$   
 200 across the two model runs and two years, scaling up by 15 (after Figure 3), and resampling to the 250 m soil grid  
 201 using bilinear interpolation.  
 202



203  
 204 **Figure 3: Modelled annual wet non-sea salt  $B_{c_{dep}}$  (Ca + Mg + K) versus measured annual  $B_{c_{dep}}$  at CAPMoN and NADP**  
 205 **stations (NADP stations limited to those within 300 m of the Canada-U.S. border). Values are averaged across two years**  
 206 **(2010 and 2016) and two model configurations. Marine station sites were corrected for sea salt contributions.**

207 The modelled  $B_{c_{dep}}$  and station observations include anthropogenic input, but the  $B_{c_{dep}}$  input to the SMB model is  
 208 meant to reflect long-term non-anthropogenic sources of base cations. However, large point sources of  $B_{c_{dep}}$  such as  
 209 the AOSR are a feature of some Canadian regions, and their impact should not be overlooked in critical load  
 210 assessments. To demonstrate the relative impact of anthropogenic sources on Canadian critical loads estimates, two  
 211 scenarios were assessed, one including anthropogenic  $B_{c_{dep}}$  and another that attempted to smooth out anthropogenic  
 212 “hot spots”.

213

214 To reduce the influence of anthropogenic point sources, a smoothing filter was applied using the SAGA GIS module  
 215 DTM Filter to identify local areas of locally intensified  $B_{c_{dep}}$ . Areas of  $B_{c_{dep}}$  above a 30% increase relative to a 20-  
 216 grid radius (approximately 50 km) were removed and infilled from their edges using inverse distance weighted





217 interpolation. Note that forest fire emissions may be substantial and appear as  $Bc_{dep}$  hot spots; for this application of  
218 the SMB, we have not added a forest fire term to the base cation budget because of the difficulty of accounting  
219 forest fire loss over the entire country.

## 220 **2.6 Soil runoff**

221 Soil runoff was obtained from the hydrological model MetHyd (Bonten et al., 2016) following Reinds et al. (2015).  
222 The data were resampled from the original resolution of  $0.1 \times 0.05^\circ$  to 250 m and gaps were infilled from the edges.  
223 A minimum  $Q$  was assigned ( $10 \text{ m}^3 \text{ ha}^{-1} \text{ yr}^{-1}$ ) for broad regions where the coarse input soil map (FAO-UNESCO,  
224 2003) used for hydrological modelling did not identify soil (i.e., exposed bedrock), but the high-resolution soil depth  
225 and texture maps used for critical loads did identify soil.

## 226 **2.7 Gibbsite equilibrium constant**

227 The gibbsite equilibrium constant ( $K_{gibb}$ ) describes the relationship between free (or unbound) aluminum  
228 concentration and pH in the soil solution. As free aluminum concentrations are generally lower in the upper organic  
229 horizons, observed ranges based on the organic matter content of the soil may be used to assign a  $K_{gibb}$  value. Soils  
230 with organic matter less than 5% were assigned a value of  $950 \text{ m}^6 \text{ eq}^{-2}$ , soils with 5–15% organic matter were  
231 assigned a lower value of  $300 \text{ m}^6 \text{ eq}^{-2} \text{ yr}^{-1}$ , and soils ranging from 15–30% organic matter were assigned a value of  
232  $100 \text{ m}^6 \text{ eq}^{-2}$  (after CLRTAP, 2015).

## 233 **2.8 Chemical criterion for damage**

234 The critical base-cation-to-aluminum ratio ( $Bc/Al_{crit}$ ) is the most widely used threshold, indicating damage to root  
235 biomass. It is a simple approach that has been used in past Canadian estimates (e.g., Carou et al., 2008). In general,  
236 it is applied as blanket or default value (e.g.,  $Bc/Al_{crit} = 1$ ) to a range of land cover types (e.g., forest or grassland).  
237 In the current study, a species- and site-specific approach was used to assign damage thresholds for forest  
238 ecosystems based on detailed tree species maps from the 2001 Canadian National Forest Inventory (NFI) (Beaudoin  
239 et al., 2014). Two levels of protection were chosen to illustrate the difference between 20% acceptable growth  
240 reduction (generally analogous to the default  $Bc/Al_{crit} = 1$ ) versus a 5% growth reduction (generally analogous to  
241  $Bc/Al_{crit} = 10$ ). Dose-response curves for  $Bc/Al_{crit}$  and root growth from Sverdrup and Warfvinge (1993) were  
242 matched to species present in the NFI database (Table 2). Values were sorted by the most sensitive species (those  
243 with the lowest  $Bc/Al_{crit}$ ) and given priority for the 250 m grid-cell value. If species-specific composition data for  
244 forests (from Beaudoin et al., 2014) were not available, the  $Bc/Al_{crit}$  value was averaged to the genus; if no genus-  
245 level data were available, an average coniferous, deciduous, or mixed forest value was applied. For non-forested  
246 soils, a default value based on a representative species for the land cover type was used (e.g., 4.5 and 0.8 for 5% and  
247 20% protection levels, respectively, for grassland based on the response of *Deschampsia*).

248

249



250 **Table 2: Species-specific  $Bc/AI_{crit}$  values for 5% and 20% growth reduction scenarios following Sverdrup & Warfvinge**  
 251 **(1993). Genus-level or generalised land cover values were derived from representative species.**

Category	$Bc/AI_{crit}$	
	5%	20%
<b>Species (forest)</b>		
<i>Abies balsamea</i>	6.0	1.1
<i>Fagus grandifolia</i>	1.3	0.6
<i>Picea mariana</i>	2.5	0.8
<i>Pseudotsuga menzerii</i>	4.0	2.0
<i>Pinus strobus</i>	1.5	0.5
<i>Picea engelmannii</i>	2.5	0.5
<i>Pinus banksiana</i>	3.0	1.5
<i>Acer saccharum</i>	1.3	0.6
<i>Alnus glutinosa</i>	4.0	2.0
<i>Quercus rubra</i>	1.3	0.6
<i>Pinus ponderosa</i>	4.5	2.0
<i>Pinus resinosa</i>	4.5	2.0
<i>Picea rubens</i>	6.0	1.2
<i>Picea sitchensis</i>	2.5	0.4
<i>Larix laricina</i>	4.0	2.0
<i>Populus tremuloides</i>	8.0	4.0
<i>Tsuga heterophylla</i>	1.0	0.2
<i>Thuja plicata</i>	1.0	0.1
<i>Betula papyrifera</i>	4.0	2.0
<i>Picea glauca</i>	2.5	0.5
<i>Betula alleghaniensis</i>	4.0	2.0
<i>Betula populifolia</i>	4.0	2.0
<i>Picea abies</i>	6.0	1.2
<i>Pinus sylvestris</i>	3.0	1.2
<b>Genus (forests)</b>		
Abies	6.0	1.1
Acer	1.3	0.6
Alnus	4.0	2.0
Betula	4.0	2.0
Fagus	1.3	0.6
Larix	4.0	2.0
Picea	2.5	0.8
Pinus	3.0	1.5
Populus	8.0	4.0
Pseudotsuga	4.0	2.0
Quercus	1.3	0.6
Thuja	1.0	0.1
Tsuga	1.0	0.2
<b>Generalised forest</b>		
Deciduous	4.0	2.0
Coniferous	3.0	1.2
Mixed	3.0	1.2
<b>Generalised land covers</b>		
Grassland	4.5	0.8
Scrubland	2.8	0.6
Tundra	2.9	0.7

252



253 **2.9 Base cation and nitrogen uptake**

254 A species- and site-specific approach was also implemented to determine the net removal of nutrients (Ca, Mg, K,  
 255 N) through tree harvesting from forest ecosystems. Base cation uptake ( $B_{c_{up}}$ ) and N uptake ( $N_{up}$ ) were estimated for  
 256 forest soils by assuming stem-only removal; site-specific stand bark and trunk biomass estimates (Beaudoin et al.,  
 257 2014) were multiplied by average trunk- and bark-specific nutrient and base cation concentration data from the tree  
 258 chemistry databases for each species present. Two ‘tree chemistry’ databases were merged to include as many tree  
 259 species as possible (U.S. data: Pardo et al., 2005; Canadian data: Paré et al., 2013); duplicate studies were removed  
 260 from the merged database and species data were averaged across studies. A simplifying assumption was made that  
 261 stand biomass was related to the species composition (i.e., the dominant tree species in a stand is also the dominant  
 262 contributor to biomass). The nutrient uptake maps were restricted to harvestable forest areas as delineated by  
 263 Dymond et al. (2010) and all other regions were set to 0. Nutrient uptake of other land types (e.g., grasslands) was  
 264 considered negligible since grazing takes place primarily in agricultural regions, which have been broadly masked  
 265 out. Since  $B_{c_{up}}$  cannot exceed inputs from deposition, weathering, and losses from leaching, a scaling factor was  
 266 used to constrain base cation uptake between its maximum (that is, deposition + weathering – leaching) and a  
 267 minimum calcium leaching value. The same scaling factor was applied to  $N_{up}$ .

268 **2.10 Denitrification fraction**

269 The soil denitrification fraction ( $f_{de}$ ) is generally related to soil drainage (CLRTAP, 2015); classes ranging from  
 270 excessive to very poor drainage were assigned using the Canada-wide Canadian Soil Information Service (CanSIS)  
 271 databases v2.2 (CLBBR, 1996) and v.3.2 (SLCWG, 2010) (Table 3). In cases of overlapping polygons from the two  
 272 databases, boundary and classification priority was given to the most recent database version before rasterization.

273  
 274 **Table 3: Denitrification fraction ( $f_{de}$ ) values (adapted from CLRTAP, 2015) and their corresponding drainage**  
 275 **classifications in versions 2.2 and 3.2 of the Canadian Soil Information Service database.**

Drainage	$f_{de}$	V2.2	V3.2
Excessive	0	E/R	VR/R
Good	0.1	W	W
Moderate	0.2	M	MW
Imperfect	0.4	I	I
Poor	0.7	P	P
Very poor	0.8	V	VP

276

277 **2.11 Deposition and exceedance**

278 Exceedances for both acidity and nutrient nitrogen were calculated against total deposition maps of annual total S  
 279 and N, which were sourced from GEM-MACH model output at 10 km horizontal grid spacing (GEM-MACH  
 280 v3.1.1.0, RAQDPS version 023) (Moran et al., 2024a, b). A three-year (2014–2016) annual average was taken to  
 281 reduce inter-annual variability in deposition, where input emissions based on annual emissions inventories specific



282 to each of these three years were used for the three annual runs. Note that Moran et al. (2024b) have presented  
283 detailed evaluations of some components of these deposition estimates, specifically ambient concentration (as a  
284 proxy for dry deposition) and wet deposition of SO<sub>2</sub> and particle sulphate (p-SO<sub>4</sub>), HNO<sub>3</sub> and p-NO<sub>3</sub>, and NH<sub>3</sub> and  
285 p-NH<sub>4</sub>, that suggest that they are robust.

286

287 Exceedances of critical load for both acidity and nutrient nitrogen (on a 250 m grid) were summarized to the 10 km  
288 deposition grid using Average Accumulated Exceedance (AAE), which is an area-weighted average that considers  
289 ecosystem coverage within each grid cell to derive the average of the summed exceedance; this addresses issues  
290 with sparse coverage and considers all ecosystems within the grid (Posch et al., 1999). The CPCAD was used to  
291 identify areas in exceedance that may be of particular concern to policymakers (ECCC, 2023b). The database,  
292 assembled in support of Canada's reporting on Canadian Environmental Sustainability Indicators and the UN  
293 Convention on Biological Diversity (among other initiatives), identifies Protected Areas (PA) such as national and  
294 provincial parks as well as Other Effective area-based Conservation Measures (OECM). Interim areas were  
295 included in expectation of their formal establishment. Areas that fell entirely within the agricultural ecumene were  
296 removed, but areas that straddled the ecumene were retained. Areas were counted as in exceedance if any part of the  
297 area experienced exceedance at the 250 m resolution.

298

299 The exceedance calculations used for acidity employed the methodology described by Posch et al. (2015), where the  
300 critical load function (Figure 2) was divided into five regions, and a different formula for exceedance was used for  
301 each region. Five inputs for each 250 m grid cell were required for these calculations: the S and N total deposition  
302 pair plus CL<sub>max</sub>S, CL<sub>min</sub>N, and CL<sub>max</sub>N values. For S and N total deposition pairs falling into four of the regions, the  
303 exceedance value will be positive (i.e., in exceedance) and its magnitude indicates how great the S and N acidic  
304 deposition at the location is above the critical load for acidity. For the Region 0, the exceedance value will be  
305 negative (i.e., not in exceedance) and its magnitude will give how far the S and N acidic deposition is below the  
306 critical load for acidity. Calculation of nutrient N exceedance was simply the difference between N<sub>dep</sub> and CL<sub>nut</sub>N.

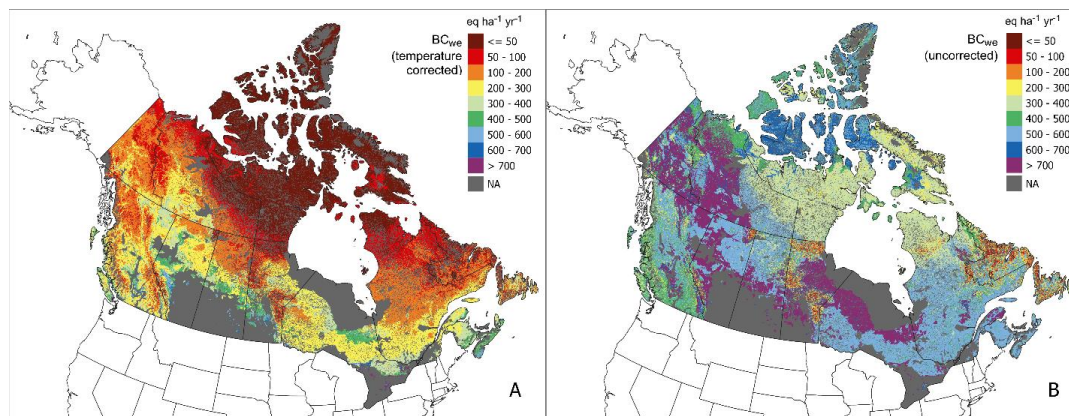
### 307 **3 Results**

#### 308 **3.1 Base cation weathering**

309 The estimate BC<sub>we</sub> was very low (below 100 eq ha<sup>-1</sup> yr<sup>-1</sup>) for nearly all regions north of 60°N latitude, and low  
310 (below 200 eq ha<sup>-1</sup> yr<sup>-1</sup>) for many northern regions south of 60°N latitude (Figure 4A). Higher BC<sub>we</sub> (above 500 eq  
311 ha<sup>-1</sup> yr<sup>-1</sup>) was predicted for the calcareous and deep soils of the Prairies and southern Ontario adjacent to agricultural  
312 regions (i.e. the mean Prairie average for natural and semi-natural soils was 714 eq ha<sup>-1</sup> yr<sup>-1</sup>), although most of these  
313 ecozones are excluded as part of the agricultural ecumene (Table 4). Average BC<sub>we</sub> for the Arctic ecozones was <  
314 50 eq ha<sup>-1</sup> yr<sup>-1</sup>, in contrast with BC<sub>we</sub> > 700 for Mixed Wood Plain and Prairie ecozones. Similarly, provincial  
315 averages were lowest for Nunavut and highest for Saskatchewan (Table 4). Base cation weathering without



316 temperature correction (Figure 4B, mean value of 570 eq ha<sup>-1</sup> yr<sup>-1</sup>) illustrates the strong effect temperature has on  
 317 limiting BC<sub>we</sub> in most of the country (average 173 eq ha<sup>-1</sup> yr<sup>-1</sup>), particularly Arctic and mountainous regions.  
 318



319  
 320 **Figure 4: Base cation weathering rate (Ca+Mg+K+Na) with temperature correction (A) and without (B). The weathering**  
 321 **rate was estimated using a soil texture approximation method with sand, clay, and parent material acid class modified by**  
 322 **depth (see Section 2.4).**

323 **Table 4: Ecozone and provincial mean values for inputs and outputs of the Simple Mass Balance model, including base**  
 324 **cation weathering (BC<sub>we</sub>), smoothed base cation deposition (BC<sub>dep</sub>), base cation uptake (BC<sub>up</sub>), nitrogen uptake (N<sub>up</sub>),**  
 325 **critical base-cation-to-aluminum ratio (Bc/Al<sub>crit</sub>) under 5% and 20% growth reduction scenarios, average sulphur**  
 326 **deposition (DepS) and nitrogen deposition (DepN) 2014 - 2017, maximum critical load of sulphur (CL<sub>max</sub>S), maximum**  
 327 **critical load of nitrogen (CL<sub>max</sub>N), minimum nitrogen critical load (CL<sub>min</sub>N) and critical load of nutrient nitrogen**  
 328 **(CL<sub>nut</sub>N). Units are in eq ha<sup>-1</sup> yr<sup>-1</sup> except for Bc/Al<sub>crit</sub> which is a unitless ratio. The critical loads presented in the table**  
 329 **were calculated using the 5% Bc/Al<sub>crit</sub> and the smoothed BC<sub>dep</sub>. Note that values represent coverage over eligible soils (e.g.**  
 330 **excluding agricultural areas and organic soils).**

Ecozone	BC <sub>we</sub>	BC <sub>dep</sub>	BC <sub>up</sub>	N <sub>up</sub>	Bc/Al <sub>crit</sub> 5%	Bc/Al <sub>crit</sub> 20%	DepS	DepN	CL <sub>max</sub> S	CL <sub>max</sub> N	CL <sub>min</sub> N	CL <sub>nut</sub> N
Arctic Cordillera	40	5	< 1	< 1	5.2	1.2	8	21	82	88	36	173
Atlantic Maritime	353	89	32	37	5.7	1.1	57	240	615	551	36	234
Boreal Cordillera	174	19	5	5	3.9	1.2	10	29	290	274	36	77
Boreal Plain	331	139	27	23	3.7	1.4	38	172	802	549	36	71
Boreal Shield	229	84	18	23	4.0	0.9	53	206	512	422	36	147
Hudson Plain	212	56	< 1	< 1	2.8	0.8	30	111	499	221	36	104
Mixedwood Plain	712	180	< 1	< 1	3.6	0.9	137	712	1586	1171	36	145
Montane Cordillera	240	52	39	42	3.6	1.2	25	98	447	473	40	164
Northern Arctic	32	7	< 1	< 1	5.6	1.3	9	20	63	75	41	75
Pacific Maritime	274	25	78	135	2.9	0.9	53	172	608	1281	48	513
Prairie	559	191	13	2	5.0	1.9	54	423	1078	893	59	63
Southern Arctic	45	21	< 1	< 1	5.6	1.3	10	26	112	118	60	65



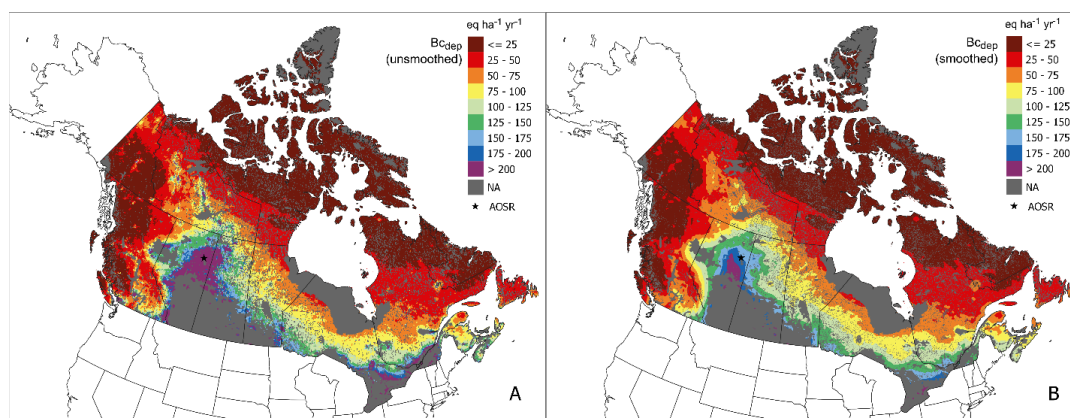
Taiga Cordillera	106	31	< 1	< 1	4.3	1.0	10	26	218	194	76	66
Taiga Plain	195	51	4	4	3.2	1.0	13	37	390	246	79	51
Taiga Shield	88	40	< 1	< 1	3.5	0.8	18	54	227	200	192	110
<b>Province</b>												
Alberta	285	133	24	17	3.7	1.4	35	142	730	512	58	78
British Columbia	235	37	40	53	3.6	1.2	26	92	439	551	91	206
Manitoba	217	86	7	7	2.9	0.9	41	146	512	338	44	66
New Brunswick	344	91	34	41	5.8	1.1	49	227	595	502	79	243
Newfoundland & Labrador	110	24	6	7	4.6	0.9	24	71	217	190	43	223
Nova Scotia	422	92	21	28	5.6	1.1	68	249	733	652	65	261
Northwest Territories	114	41	< 1	< 1	4.0	1.0	11	28	254	191	36	49
Nunavut	34	11	< 1	< 1	5.5	1.2	9	22	75	87	36	75
Ontario	306	103	23	19	3.8	0.9	61	289	666	509	66	141
Prince Edward Island	422	69	19	18	5.3	1.0	57	209	672	558	66	226
Québec	148	46	11	14	4.5	1.0	38	132	314	299	50	153
Saskatchewan	230	124	12	8	3.1	1.0	29	128	607	492	49	62
Yukon	148	25	< 1	< 1	3.8	1.0	10	26	266	233	36	54
<b>Canada</b>	<b>132</b>	<b>52</b>	<b>8.2</b>	<b>10</b>	<b>4.5</b>	<b>1.1</b>	<b>76</b>	<b>22</b>	<b>291</b>	<b>258</b>	<b>48</b>	<b>99</b>

331

### 332 3.2 Base cation deposition

333 Modelled  $B_{c,dep}$  ranged from low ( $< 25 \text{ eq ha}^{-1} \text{ yr}^{-1}$ ) in the north to higher values ( $> 200 \text{ eq ha}^{-1} \text{ yr}^{-1}$ ) around the  
 334 Prairies and the southern regions of the eastern provinces (Figure 5) as well as in Alberta and Saskatchewan (Table  
 335 4). Average (smoothed)  $B_{c,dep}$  was roughly one-third of  $BC_{we}$ . Hot spots of  $BC_{dep}$  associated with anthropogenic  
 336 point sources (e.g., from mining operations as well as the contribution from the AOSR) were clearly visible in the  
 337 unsmoothed map (Figure 5A). The smoothing algorithm (Figure 5B) eliminated most of the effects of point sources,  
 338 at the cost of some loss of definition (Canada-wide average of  $52 \text{ eq ha}^{-1} \text{ yr}^{-1}$  pre-smoothing and  $68 \text{ eq ha}^{-1} \text{ yr}^{-1}$  post-  
 339 smoothing). However, it did not completely erase elevated  $B_{c,dep}$  in the AOSR; the difference in size between other  
 340 point source footprints and the AOSR necessitated a compromise in filter radius and slope selection.



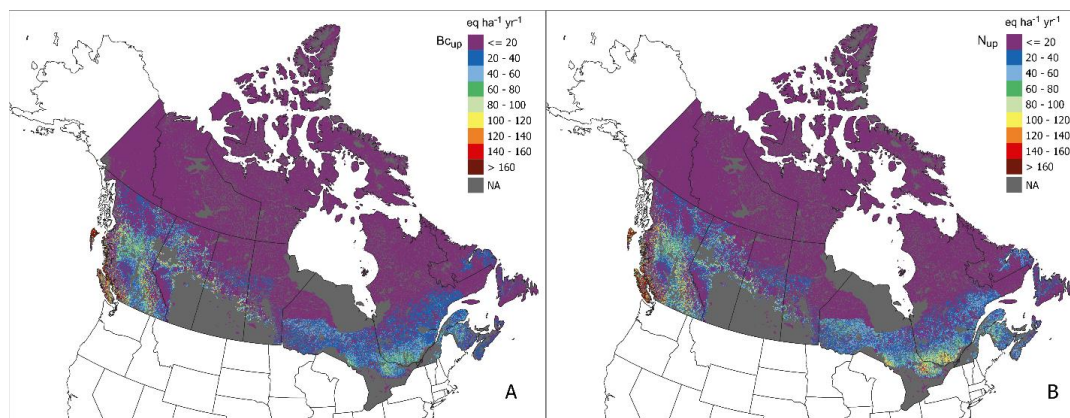


341

342 **Figure 5: Non-sea-salt base cation deposition (Ca + Mg + K) with anthropogenic contributions (A) and after a smoothing**  
 343 **filter was applied to reduce the effect of anthropogenic point sources (B). The Athabasca Oil Sands Region (AOSR) is**  
 344 **identified by a star.**

345 **3.3 Base cation and nitrogen uptake**

346 Base cation uptake ranged from  $< 1$  to  $545 \text{ eq ha}^{-1} \text{ yr}^{-1}$  and was highest in coastal British Columbia; the Pacific  
 347 Maritime ecozone had the highest mean  $B_{c,up}$  at  $79 \text{ eq ha}^{-1} \text{ yr}^{-1}$  (Table 4). Nitrogen uptake was also high in British  
 348 Columbia and the Pacific Maritime zone (mean  $N_{up}$  of  $135 \text{ eq ha}^{-1} \text{ yr}^{-1}$ ) as well as the Montane Cordillera (mean  $N_{up}$   
 349 of  $42 \text{ eq ha}^{-1} \text{ yr}^{-1}$ ). Regions of elevated  $N_{up}$  were seen in eastern Ontario and southern Quebec (Figure 6); these occur  
 350 on the Boreal Shield ecozone, which is a large ecozone that extends across multiple provinces over which  $N_{up}$  varies  
 351 (but with a mean value of  $23 \text{ eq ha}^{-1} \text{ yr}^{-1}$ ).



352

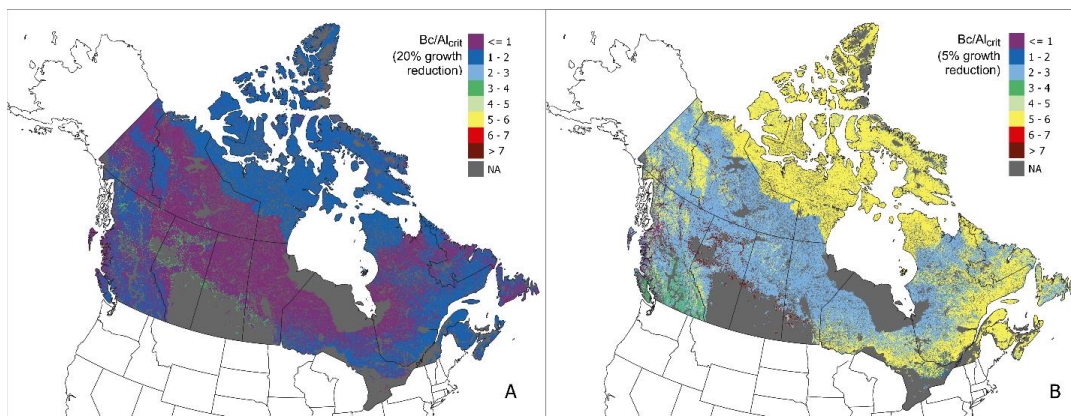
353 **Figure 6: Base cation (Ca+Mg+K) uptake (A) and nitrogen uptake (B); forested regions limited to harvestable regions**  
 354 **(identified by Dymond et al. (2010)). Uptake for non-forested ecosystems was set to 0.**

355 **3.4 Critical base-cation-to-aluminum ratio**

356 Almost the entire country fell below a  $B_c/Al_{crit}$  ratio of 2 under 20% root biomass growth reduction (Figure 7A). In  
 357 contrast, a  $B_c/Al_{crit}$  ranged from 1–8 (average = 4.4) under the 5% root biomass growth reduction (Figure 7B). The  
 358 ratio ranged from 3–6 for forests in eastern Canada (A and B ecozones), while ranges for the Boreal Shield ecozone



359 were 2–4 and coastal forest in British Columbia were slightly higher at 3–4. Semi-natural grassland in the Prairies  
 360 were given a ratio of 4.5 based on *Deschampsia*, but many fringe regions of the Prairies are treed and dominated by  
 361 *Populus tremuloides*, which had a  $Bc/Al_{crit}$  of 8.

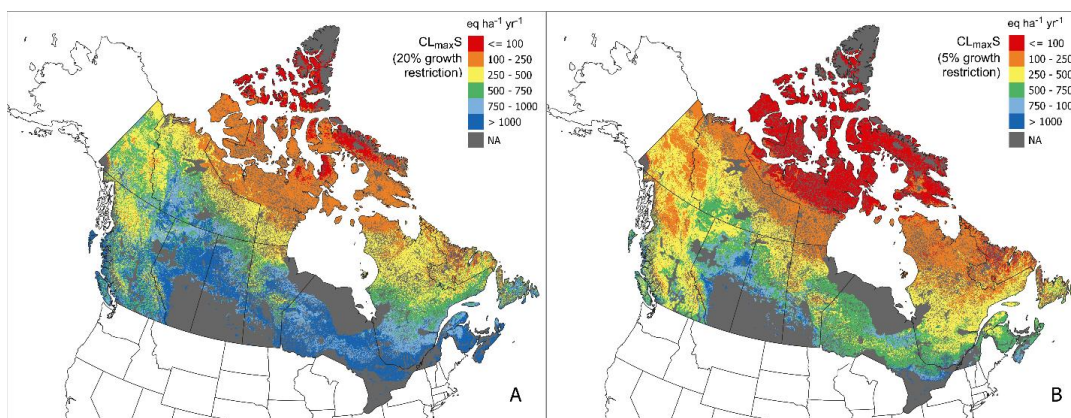


362  
 363 **Figure 7: Critical base-cation-to-aluminum ratio ( $Bc/Al_{crit}$ ) under a 20% growth reduction (A) and a 5% growth**  
 364 **reduction (B). Site-specific ratios were selected for each 250 m grid cell for the most sensitive species (or genus or land-**  
 365 **cover type if no species data available). Note that while the legends have been matched for comparison, the maximum**  
 366 **ratio in the 20% growth reduction map is 4.**

### 367 3.5 Critical loads

368 The  $CL_{maxS}$  under the 20% protection level (i.e., allowing more damage) showed low sensitivity ( $> 1000 \text{ eq ha}^{-1} \text{ yr}^{-1}$ )  
 369 to acidic deposition for most regions below  $55^\circ\text{N}$  latitude (Figure 8A). In contrast, under the 5% protection level  
 370 (Figure 8B), low sensitivity was limited to southern agricultural regions in the Prairies. Lowest  $CL_{maxS}$  and  $CL_{maxN}$   
 371 were found in the Arctic territories (Nunavut, the Northwest Territories, the Yukon; Table 4) and also  
 372 Newfoundland and Labrador (Figure 12B). Of the provinces, Quebec had the lowest  $CL_{maxS}$  ( $314 \text{ eq ha}^{-1} \text{ yr}^{-1}$ ) and  
 373  $CL_{maxN}$  ( $299 \text{ eq ha}^{-1} \text{ yr}^{-1}$ ) (Table 4).

374



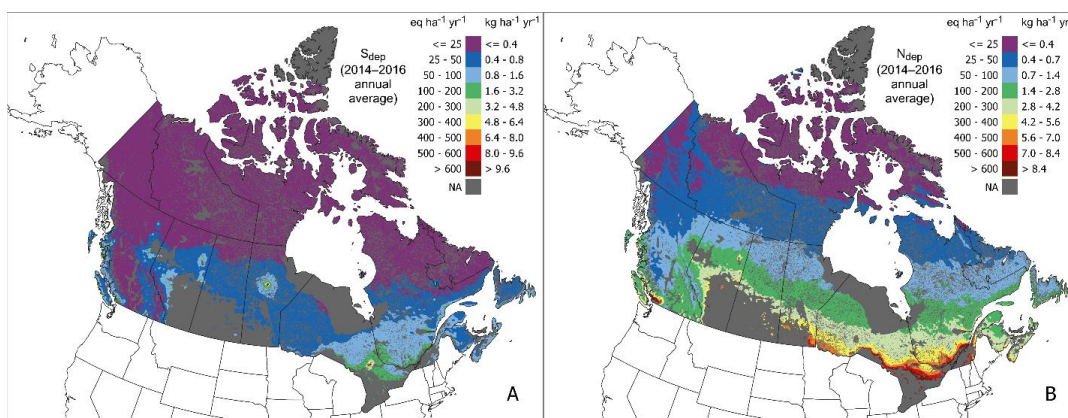
375  
 376 **Figure 8: Maximum sulphur critical load ( $CL_{maxS}$ ) at a 20% growth restriction scenario (A) versus a 5% growth**  
 377 **restriction scenario (B), using reduced-anthropogenic (i.e., smoothed)  $Bc_{dep}$ .**





378 **3.6 Deposition**

379 Modelled average annual  $S_{dep}$  was below 25 eq ha<sup>-1</sup> yr<sup>-1</sup> for most of the country above 59°N, as well as the Montaine  
 380 Cordillera ecozone that covers much of British Columbia (Figure 9A). Southern Quebec and central Ontario  
 381 showed higher annual average values between 50–200 eq ha<sup>-1</sup> yr<sup>-1</sup>, with some isolated point sources showing  $S_{dep}$  in  
 382 excess of 500 eq ha<sup>-1</sup> yr<sup>-1</sup>. Modelled average annual  $N_{dep}$  (Figure 9B) exceeded  $S_{dep}$  in most parts of the country.  
 383 Nitrogen deposition exceeding 500 eq ha<sup>-1</sup> yr<sup>-1</sup> was present in northern Ontario and southern Quebec as well as  
 384 southern Manitoba and southwestern British Columbia.



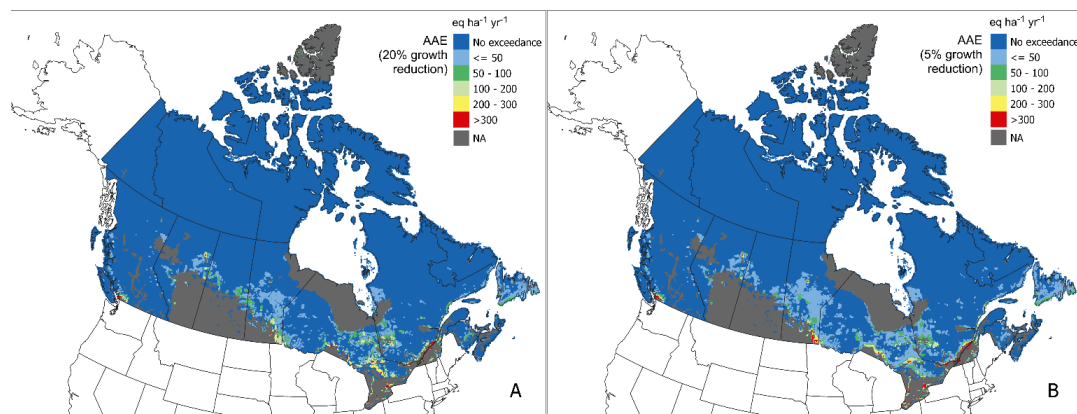
385  
 386 **Figure 9: Modelled total deposition of sulphur ( $S_{dep}$ , panel A) and nitrogen ( $N_{dep}$ , panel B) under average annual**  
 387 **deposition from 2014–2016. Maps were sourced from GEM-MACH (Moran et al., 2024a, b).**

388 **3.7 Exceedances**

389 Widespread but low exceedances of acidity (< 50 eq ha<sup>-1</sup> yr<sup>-1</sup>) under 2014–2016 deposition were found in regions in  
 390 central and southern Quebec, Ontario, Manitoba, Alberta, British Columbia as well as in some regions in Nova  
 391 Scotia and Newfoundland, under both protection levels (Figure 10). Further, exceedances above 200 eq ha<sup>-1</sup> yr<sup>-1</sup>  
 392 were predicted in southern Quebec and Ontario, as well as near Winnipeg and Vancouver, under both protection  
 393 levels. Exceedances of acidity under 2014–2016 S and N deposition were not generally predicted in the north. The  
 394 spatial extent of exceedance was slightly greater under the 5% protection limit as a result of higher  $CL_{max}S$  and  
 395  $CL_{max}N$ , particularly around point sources of S and N, such as the AOSR.

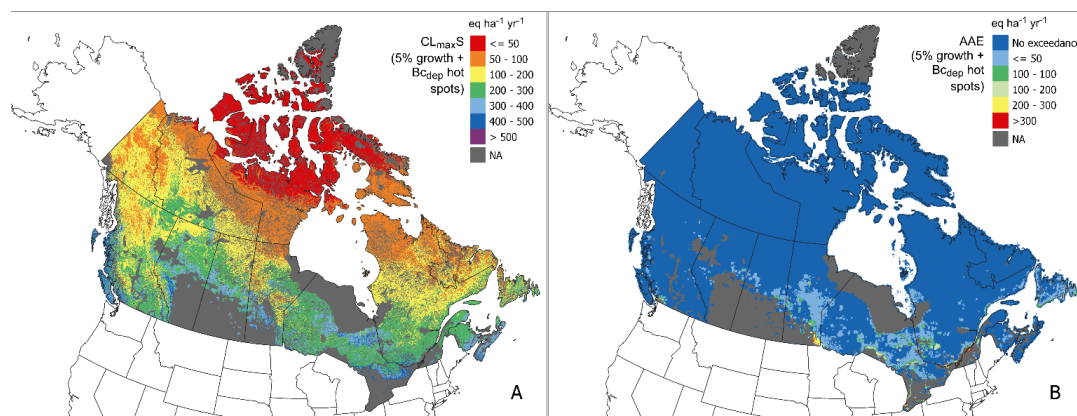
396  
 397 If the  $Bc_{dep}$  without smoothing is employed (i.e., the base cation deposition associated with high magnitude  
 398 anthropogenic sources is included), exceedances are reduced (see Figure 11(B) and compare to Figure 10(B)). The  
 399  $CL_{max}S$  based on anthropogenic-inclusive  $Bc_{dep}$  (at 5% protection level, Figure 11A) indicated that  $CL_{max}S$  is  
 400 elevated in the AOSR in comparison with the smoothed  $CL_{max}S$  in Figure 8B.

401



402

403 **Figure 10: Average Accumulated Exceedance (AAE) of critical loads of acidity under 2014–2016 sulphur plus nitrogen**  
 404 **GEM-MACH modelled deposition. Two growth reduction scenarios are presented: using a chemical criterion**  
 405 **representing 20% growth reduction (A) and 5% growth reduction (B).**



406

407 **Figure 11: A scenario including base cation deposition without smoothing, illustrating the impact of hot-spot**  
 408  **$Bc_{dep}$  on the maximum critical load of sulphur ( $CL_{maxS}$ ) (A) and the Average Accumulated Exceedance (AAE) under 2014–2016**  
 409 **sulphur plus nitrogen GEM-MACH modelled deposition (B).**

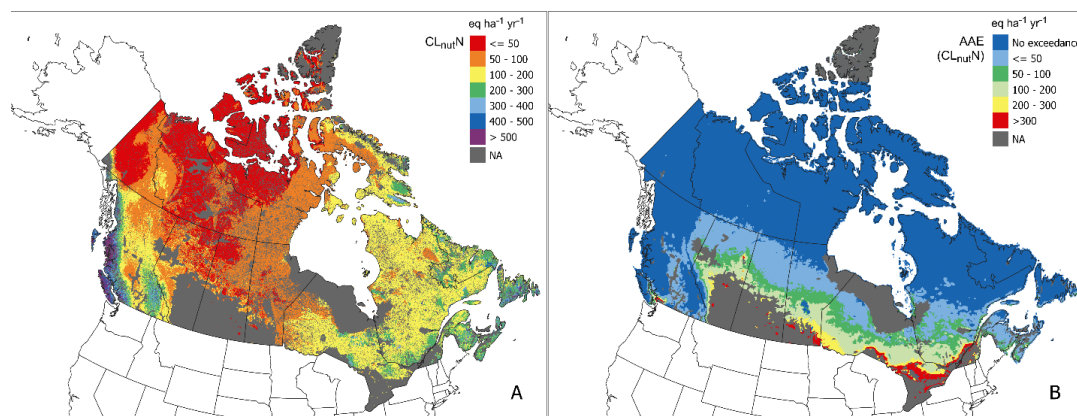
410 For  $CL_{nutN}$ , central and northern regions of the country were sensitive to nutrient N deposition, particularly pastures,  
 411 grasslands, scrublands, and sparse forest in and surrounding the Prairies (Figure 12A). Further, very low  $CL_{nutN}$  ( $\leq$   
 412  $75 \text{ eq ha}^{-1} \text{ yr}^{-1}$ ) were estimated over the Arctic territories (Table 4) as well as in northern Alberta and the Athabasca  
 413 Basin in northern Saskatchewan (Figure 12A). Widespread exceedances of  $CL_{nutN}$  were predicted across most  
 414 provinces, with generally low AAE ( $< 50 \text{ eq ha}^{-1} \text{ yr}^{-1}$ ) extending to just north of  $60^\circ$  latitude, and higher values of  
 415  $100\text{--}200 \text{ eq ha}^{-1} \text{ yr}^{-1}$  were predicted from Alberta east to Quebec (Figure 12B). Some regions adjacent to the  
 416 agricultural ecumene in the Prairies, southern Ontario, Quebec and the AOSR experienced values above  $300 \text{ eq ha}^{-1}$   
 417  $\text{yr}^{-1}$  (Figure 12B).

418

419 There were 12,341 sites of interest across Canada (i.e., PA and OECM areas); however, only 8,372 fall within areas  
 420 assessed in this study (e.g. not within the agricultural ecumene or Hudson Bay Plains ecozone). In total, 10% of



421 these sites exceeded  $CL_{max}S$  under the 5% protection limit (Table 5). This was roughly double the number of sites in  
 422 exceedance under the 20% protection limit. By comparison the  $Bc_{dep}$  layer with unsmoothed hot spots (i.e. retaining  
 423 higher  $Bc_{dep}$  close to anthropogenic emissions areas) under the 5% protection limit showed a reduction in total areas  
 424 that are in exceedance of acidity critical loads; anthropogenic emissions of base cations reduce the exceedances by  
 425 reducing  $N_{up}$  values. The number of PA and OECM sites in exceedance of  $CL_{nut}N$  was much higher, 70% of total  
 426 sites assessed (Table 5).



427  
 428 Figure 12: Critical load of nutrient nitrogen using the SMB model (A) and average accumulated exceedance of  
 429 nutrient nitrogen (B) estimated under modelled total deposition of nitrogen from 2014–2016.

430

431 **Table 5: Exceedance summarized by number of Protected Areas (PA) and Other Effective area-based Conservation**  
 432 **Measures (OECM) areas (ECCC, 2023b) experiencing any exceedance. Three exceedance scenarios are presented:**  
 433 **Critical load of acidity exceedance at 5% and 20% growth reduction protection levels, unsmoothed base cation deposition**  
 434 **under the 5% scenario, and exceedance of nutrient nitrogen ( $CL_{nut}N$ ). Critical loads of acidity and nutrient nitrogen**  
 435 **were assessed under a multi-year (2014–2016) average GEM-MACH modelled sulphur and nitrogen total deposition.**

	PA	OECM	% Exceeded
Number of sites	8,205	167	-
Exceeded (5% growth reduction)	793	17	9
Exceeded (20% growth reduction)	313	10	3
Exceeded (5% with hot spots)	445	14	5
Exceeded ( $CL_{nut}N$ )	5,807	85	70

436

## 437 4 Discussion

### 438 4.1 Uncertainties of critical loads of acidity and nutrient nitrogen

439 Critical loads of acidity reflect the influence of  $BC_{we}$ , particularly in the north where cold annual temperatures slow  
 440 weathering rates to almost zero. However, areas near the Canada-U.S. border also showed lower  $BC_{we}$  rates by 200–  
 441 300  $eq\ ha^{-1}\ yr^{-1}$  when corrected for temperature (Figure 4). Soil depth remains a poorly mapped parameter that has  
 442 significant impact on  $BC_{we}$ , and it is worth noting that average estimates were based on mapped soil depths (Hengl,



443 2017), which ranged from 1 cm to a maximum rooting depth of 30 or 50 cm. While comparison between mapped  
444 values and site-level values is difficult (due to methodological differences and spatial representation), there are some  
445 studies which have observational values in representative areas; for example, in northern Saskatchewan, 50% of 107  
446 sites were estimated below 300 eq ha<sup>-1</sup> yr<sup>-1</sup>, slightly above our mapped estimates of 230 eq ha<sup>-1</sup> yr<sup>-1</sup> for (primarily  
447 northern) Saskatchewan (Table 4; Figure 4). Estimates for conifer stands in Québec by Ouimet et al. (2001) were  
448 210 eq ha<sup>-1</sup> yr<sup>-1</sup>, comparable to the mean 229 eq ha<sup>-1</sup> yr<sup>-1</sup> estimated for the Boreal Shield ecozone in our study (Table  
449 4). In British Columbia, Mongeon et al. (2010) found BC<sub>we</sub> to be 710 eq ha<sup>-1</sup> yr<sup>-1</sup>, much greater than the 235 eq ha<sup>-1</sup>  
450 yr<sup>-1</sup> estimated in our study for the Pacific Maritime ecozone. Koseva et al., (2010) estimated BC<sub>we</sub> at 10 sites in  
451 Ontario primarily in the Mixedwood Plains ecozone at 628 eq ha<sup>-1</sup> yr<sup>-1</sup> (compared to 306 eq ha<sup>-1</sup> yr<sup>-1</sup> over the  
452 Mixedwood Plains in our study). Moreover, Koseva et al. suggest that the soil-texture approximation method (as  
453 used in our study) under-estimates BC<sub>we</sub> in comparison to the better-performing PROFILE model. Assessments of  
454 uncertainty in critical load estimates recognize BC<sub>we</sub> as the primary driver of uncertainty (Li and McNulty, 2007;  
455 Skeffington et al., 2006) and, as such, observational data and PROFILE-modelled site data to constrain weathering  
456 rates would greatly improve critical load estimates.

457

458 While the inclusion of a modelled B<sub>cdep</sub> map represents an improvement over previous Canadian critical load map  
459 projects, several factors likely contribute to the B<sub>cdep</sub> modelled negative bias (which has appeared in other  
460 publications, such as Makar et al., 2018), and may relate to how emissions processing has been carried out for air-  
461 quality models in North America. While anthropogenic emissions inventories include estimates of PM<sub>2.5</sub>, PM<sub>10</sub> and  
462 PM<sub>total</sub> mass emissions, usually only PM<sub>2.5</sub> and PM<sub>10</sub> emissions are used in determination of model input emissions.  
463 However, substantial emitted base cation mass may reside in the larger size fractions (between the mass included  
464 within PM<sub>10</sub> and the PM<sub>total</sub>). The model version and emissions inventory data used in the base cation deposition  
465 estimates of AQMEII4 included only emissions up to 10 µm diameter, as did work examining emissions from  
466 multiple sources of primary particulate matter (Boutzis et al., 2020). Subsequent work using observations from the  
467 Canadian Oil Sands and reviewing other sources of data subsequent to Boutzis et al. (2020) and Galmarini et al.  
468 (2021) suggest that many of the same sources of anthropogenic particulate matter emissions include emitted  
469 particles between 10 and 40 µm diameter, the mass of which adds an additional 66% relative to the PM<sub>2.5</sub> to PM<sub>10</sub>  
470 “coarse mode” emitted mass. For forest fire emissions, this additional mass is much larger. The wildfire particulate  
471 matter size distributions of Radke et al. (1988; 1990) used to estimate mass up to PM<sub>10</sub> in Boutzis et al. (2020) show  
472 that the emitted particle mass between 10 and 40 µm diameter is 7.26× that emitted between PM<sub>2.5</sub> and PM<sub>10</sub>.  
473 Approximately 9.7% of this particle mass is composed of base cations (e.g., Table S5 of Chen et al., 2019). A third  
474 factor is another natural emissions source, aeolian or wind-blown dust emissions (e.g., Bullard et al., 2016; Park et  
475 al., 2010), which was not included in the AQMEII4 simulations. These (traditionally missing) sources of base  
476 cation mass in air-quality models likely contribute to the substantial negative bias noted here. Nevertheless,  
477 regression in Figure 3 suggests that the spatial distribution of base cations emissions and deposition from Galmarini  
478 et al. (2021) is reasonable, and we have used the relationship between modelled and observed values to provide  
479 corrected estimates of B<sub>cdep</sub>.



480

481 The conservative 5% protection level set for the  $Bc/Al_{crit}$  is favoured by the authors of the current work for critical  
482 loads estimates, which affords greater ecosystem protection consistent with studies using  $Bc/Al > 1$  (e.g. McDonnell  
483 et al., 2023; Mongeon et al., 2010; Ouimet et al., 2006). Historically, when acidic deposition was higher than at  
484 present, a 20% growth reduction was a reasonable target. However, under decreasing emissions and deposition, as  
485 well as acceptable impacts to wood production, carbon storage, and ecosystem health there is greater certainty in  
486 ecosystem protection under the 5% protection level. It should be noted that the level of protection is an ethical  
487 choice regarding how much should be protected, rather than a sensitivity, and taking the most sensitive species  
488 through the  $Bc/Al_{crit}$  selection process ensures the highest possible protection based on species-specific dose-  
489 response curves. Note, however, that changes to forest health and climate may also induce pressures that are not  
490 captured in the selection of the  $Bc/Al_{crit}$  from the studies described in Sverdrup & Warfvinge (1993).

491 Low  $CL_{nutN}$  in the Arctic was driven by very low  $Q$  values on thin barren land covers. In contrast, areas with high  
492  $Q$  were found to result in high  $CL_{nutN}$ ; as previously suggested by Reinds et al. (2015), a critical flux rather than  
493 concentration may provide more reliable critical loads in regions with elevated precipitation such as the Pacific  
494 Maritime ecozone in British Columbia.

495

496 The omission of wetlands, which cover an estimated 13% of land in Canada, from acidity and nutrient N critical  
497 loads represents a gap in terrestrial (and aquatic) ecosystem protection. Although there are modifications to the  
498 SMB model that address critical loads for wetlands, this study was limited by the availability of a suitable national  
499 wetlands classification map. Future studies may address this data gap as wetland classification products become  
500 available.

#### 501 **4.2 Exceedances of critical loads**

502 Historically, forests in eastern Canada were regarded as the region most susceptible to acidification due to their  
503 underlying geology, shallow soil type, vegetation, and elevated acidic deposition from domestic and transboundary  
504 air pollution. This study adds to the body of literature supporting recent studies in both terrestrial and aquatic  
505 critical loads (e.g., Makar et al., 2018; Cathcart et al., 2016; Williston et al., 2016; Mongeon et al., 2010; Whitfield  
506 et al., 2010), showing likely exceedance of critical loads of acidity in central and western Canada (i.e., in regions  
507 such as Alberta, Saskatchewan and British Columbia). The prevalence of our predicted widespread exceedances in  
508 Manitoba (Figure 10) may reflect low mineral soil depth, as organic soil dominates this part of the country. Further,  
509 point sources (generally large mining or smelting operations) remain a concern (e.g., in southern Manitoba, the  
510 AOSR, and southern British Columbia) with regard to sharply elevated local exceedance, which may be temporally  
511 mitigated by elevated  $Bc_{dep}$  from co-located dust emissions sources. Additionally, high  $Bc_{dep}$  can have an  
512 alkalinizing impact on ecosystems. In China, where elevated  $Bc_{dep}$  emissions from industrialization have  
513 historically mitigated the effects of acidic deposition in many regions, successful particle emissions mitigation  
514 strategies have reduced  $Bc_{dep}$  in recent years (as S and N deposition have declined), resulting in increased critical  
515 load exceedance (Zhao et al., 2021). However, the steady-state assumptions of the SMB require non-anthropogenic





516  $B_{c,dep}$ , since they must reflect long-term conditions, and base cation emissions cannot be reliably coupled with  
517 changes to those of S and N and should be considered separately.

518

519 Widespread  $CL_{nut}N$  exceedance (found in the majority of the PA and OECM sites assessed) suggests that nutrient N  
520 may present a risk to biodiversity at many sites under protective measures. While some empirical studies of nutrient  
521 N have been done in Canada, a large knowledge gap exists for many Canadian ecosystems regarding the effect of  
522 nutrient nitrogen and their critical loads. Some work has developed on Jack Pine and northern ecosystems;  
523 Vandinther suggested that across Jack pine-dominant forests surrounding the AOSR, the biodiversity-based  
524 empirical critical load of nutrient N was  $5.6 \text{ kg ha}^{-1} \text{ yr}^{-1}$  ( $400 \text{ eq ha}^{-1} \text{ yr}^{-1}$ ; Vandinther and Aherne, 2023a) which  
525 is above the maximum  $CL_{nut}N$  calculated in this study within 200 km of the AOSR ( $216 \text{ eq ha}^{-1} \text{ yr}^{-1}$ ). Further, in low  
526 deposition ‘background’ regions a biodiversity-based empirical critical load of  $1.4\text{--}3.15 \text{ kg ha}^{-1} \text{ yr}^{-1}$  ( $100\text{--}225 \text{ eq}$   
527  $\text{ha}^{-1} \text{ yr}^{-1}$ ) was found to protect lichen communities and other N-sensitive species in Jack pine forests across  
528 Northwestern Canada (Vandinther and Aherne, 2023b); these are again higher compared to mean values in this  
529 study (e.g. for the Boreal Plain,  $76 \text{ eq ha}^{-1} \text{ yr}^{-1}$ ). Empirical critical loads developed for ecoregions in Northern  
530 Saskatchewan (Murray et al., 2017) fall into a range of  $88\text{--}123 \text{ eq ha}^{-1} \text{ yr}^{-1}$ , again higher than values suggested by  
531 this study (e.g.  $62 \text{ eq ha}^{-1} \text{ yr}^{-1}$  in Saskatchewan). While the spatial pattern of  $CL_{nut}N$  exceedances does not generally  
532 follow exceedances of critical loads of acidity, some areas (including PA and OECM sites) in central Canada were  
533 estimated to be in exceedance of both critical loads of acidity and nutrient N, suggesting that this region may be of  
534 particular concern.

## 535 **5 Conclusions**

536 This study mapped critical loads of acidity and nutrient nitrogen for terrestrial ecosystems the using the steady-state  
537 SMB model. The modelling approach used (a) high-resolution national maps of soils, meteorology, and forest  
538 composition, (b) high-resolution modelled Canada-wide  $B_{c,dep}$ , and (c) species-specific chemical criteria for damage.  
539 The resulting national critical loads of acidity and nutrient N for Canadian terrestrial ecosystems were mapped at a  
540 250 m resolution. The influence of different levels of protection and  $B_{c,dep}$  models to several parameters was also  
541 explored, including two vegetation protection levels (5% and 20% root biomass growth reduction scenarios) and  
542 anthropogenic base cation deposition “hot spots”.

543

544 Terrestrial ecosystems in Canada continue to receive acidic deposition in excess of their critical loads for both  
545 acidity and nutrient N under modelled (2014–2016) total S and N deposition in areas of both eastern and western  
546 Canada. These areas include several major point emissions sources including the Alberta Oil Sands Region.  
547 Further, exceedance was predicted at 10% (acidity) and 70% (nutrient nitrogen) of the assessed sites (PA and  
548 OECM) where preserving biodiversity is a national policy goal, suggesting that current levels of N deposition may  
549 be affecting a large majority of these ecologically important sites. Soil recovery from acidic deposition is a slow  
550 process that may take decades or even centuries to reach pre-acidification levels, which cannot begin until  
551 deposition falls below critical loads. Parameterization of the SMB model specifically for Canadian ecosystems is a



552 step forward in refining Canadian terrestrial critical loads, and the maps produced by this study are a valuable tool in  
553 identifying and assessing regions sensitive to acidic deposition and nutrient N deposition, as well they provide a  
554 foundation for more refined provincial estimates.

#### 555 **CRedit authorship contribution statement**

556 **H. Cathcart:** Conceptualization, Data curation, Investigation, Methodology, Formal analysis, Visualization, Writing  
557 – original draft, Writing – review & editing. **J. Aherne:** Formal analysis, Methodology, Writing – review &  
558 editing. **M.D. Moran:** Data curation, Investigation, Methodology, Writing – original draft, Writing – review &  
559 editing. **V. Savic-Jovicic:** Data curation, Investigation. **P.A. Makar:** Investigation, Methodology, Writing – original  
560 draft, Writing – review & editing. **A.D Cole:** Writing – review & editing.

#### 561 **Competing interests**

562 The authors declare that they have no conflict of interest.

#### 563 **Data availability**

564 Raster files of critical load maps ( $CL_{maxS}$ ,  $CL_{maxN}$ ,  $CL_{minN}$ ,  $CL_{nutN}$ ) will be made available on the Government of  
565 Canada's Open Data Portal under Environment and Climate Change Canada's records  
566 (<https://open.canada.ca/data/organization/ec>).

#### 567 **Acknowledgements**

568 This study was funded by Environment and Climate Change Canada. The authors wish to acknowledge Max Posch  
569 for his provision of (and guidance regarding) soil water runoff (Q) estimates, and the AQMEI4 project for  
570 emissions data leading to GEM-MACH maps of base cation deposition.

#### 571 **References**

- 572 Agriculture and Agri-Food Canada: Terrestrial Ecozones of Canada [dataset], [https://open.canada.ca/data/en/dataset/7ad7ea01-](https://open.canada.ca/data/en/dataset/7ad7ea01-eb23-4824-bccc-66adb7c5bdf8)  
573 [eb23-4824-bccc-66adb7c5bdf8](https://open.canada.ca/data/en/dataset/7ad7ea01-eb23-4824-bccc-66adb7c5bdf8), 2013.
- 574 Aherne, J. and Posch, M.: Impacts of nitrogen and sulphur deposition on forest ecosystem services in Canada, *Curr. Opin.*  
575 *Environ. Sustain.*, 5, 108–115, <https://doi.org/10.1016/j.cosust.2013.02.005>, 2013.
- 576 Aklilu, Y.-A., Blair, L., Dinwoodie, G., and Aherne, J.: Using steady-state mass balance model to determine critical loads of  
577 acidity for terrestrial ecosystems in Alberta, Government of Alberta, Ministry of Environment and Parks, 2022.
- 578 Beaudoin, A., Bernier, P. Y., Guindon, L., Villemaire, P., Guo, X. J., Stinson, G., Bergeron, T., Magnussen, S., and Hall, R. J.:  
579 Mapping attributes of Canada's forests at moderate resolution through kNN and MODIS imagery, *Can. J. For. Res.*, 44, 521–532,  
580 <https://doi.org/10.1139/cjfr-2013-0401>, 2014.



- 581 Bobbink, R. and Hicks, W. K.: Factors Affecting Nitrogen Deposition Impacts on Biodiversity: An Overview, in: Nitrogen  
582 Deposition, Critical Loads and Biodiversity, edited by: Sutton, M. A., Mason, K. E., Sheppard, L. J., Sverdrup, H., Haeuber, R.,  
583 and Hicks, W. K., Springer Netherlands, Dordrecht, 127–138, [https://doi.org/10.1007/978-94-007-7939-6\\_14](https://doi.org/10.1007/978-94-007-7939-6_14), 2014.
- 584 Bobbink, R., Loran, C., and Tomassen, H.: Review and revision of empirical critical loads of nitrogen for Europe,  
585 Umweltbundesamt/German Environment Agency, Dessau-Roßlau, Germany, 2022.
- 586 Bonten, L. T. C., Reinds, G. J., and Posch, M.: A model to calculate effects of atmospheric deposition on soil acidification,  
587 eutrophication and carbon sequestration, *Environ. Model. Softw.*, 79, 75–84, <https://doi.org/10.1016/j.envsoft.2016.01.009>, 2016.
- 588 Boutzis, E. I., Zhang, J., and Moran, M. D.: Expansion of a size disaggregation profile library for particulate matter emissions  
589 processing from three generic profiles to 36 source-type-specific profiles, *J. Air Waste Manag. Assoc.*, 70, 1067–1100,  
590 <https://doi.org/10.1080/10962247.2020.1743794>, 2020.
- 591 Bouwman, A. F., Vuuren, D. P. V., Derwent, R. G., and Posch, M.: A Global Analysis of Acidification and Eutrophication of  
592 Terrestrial Ecosystems, *Water. Air. Soil Pollut.*, 141, 349–382, 2002.
- 593 Bullard, J. E., Baddock, M., Bradwell, T., Crusius, J., Darlington, E., Gaiero, D., Gassó, S., Gisladottir, G., Hodgkins, R.,  
594 McCulloch, R., McKenna-Neuman, C., Mockford, T., Stewart, H., and Thorsteinsson, T.: High-latitude dust in the Earth system,  
595 *Rev. Geophys.*, 54, 447–485, <https://doi.org/10.1002/2016RG000518>, 2016.
- 596 Burns, D. A., Blett, T., Haeuber, R., and Pardo, L. H.: Critical loads as a policy tool for protecting ecosystems from the effects of  
597 air pollutants, *Front. Ecol. Environ.*, 6, 156–159, <https://doi.org/10.1890/070040>, 2008.
- 598 Carou, S., Dennis, I., Aherne, J., Ouimet, R., Arp, P. A., Watmough, S. A., DeMerchant, I., Shaw, M., Vet, B., Bouchet, V., and  
599 Moran, M.: A national picture of acid deposition critical loads for forest soils in Canada, Canadian Council of Ministers of the  
600 Environment, Winnipeg, Manitoba, 2008.
- 601 Cathcart, H., Aherne, J., Jeffries, D. S., and Scott, K. A.: Critical loads of acidity for 90,000 lakes in northern Saskatchewan: A  
602 novel approach for mapping regional sensitivity to acidic deposition, *Atmos. Environ.*, 146, 290–299,  
603 <https://doi.org/10.1016/j.atmosenv.2016.08.048>, 2016.
- 604 CEC: 2010 Land Cover of North America at 250 meters (v2.0) [dataset], Commission for Environmental Cooperation (CEC).  
605 Canada Centre for Remote Sensing (CCRS), U.S. Geological Survey (USGS), Comisión Nacional para el Conocimiento y Uso de  
606 la Biodiversidad (CONABIO), Comisión Nacional Forestal (CONAFOR), Instituto Nacional de Estadística y Geografía (INEGI),  
607 2018.
- 608 Chen, J., Anderson, K., Pavlovic, R., Moran, M. D., Englefield, P., Thompson, D. K., Munoz-Alpizar, R., and Landry, H.: The  
609 FireWork v2.0 air quality forecast system with biomass burning emissions from the Canadian Forest Fire Emissions Prediction  
610 System v2.03, *Geosci. Model Dev.*, 12, 3283–3310, <https://doi.org/10.5194/gmd-12-3283-2019>, 2019.
- 611 Clark, C. M., Morefield, P. E., Gilliam, F. S., and Pardo, L. H.: Estimated losses of plant biodiversity in the United States from  
612 historical N deposition (1985–2010), *Ecology*, 94, 1441–1448, <https://doi.org/10.1890/12-2016.1>, 2013.
- 613 CLBBR: Soil Landscapes of Canada, v. 2.2 [dataset], Centre for Land and Biological Resources Research. Research Branch,  
614 Agriculture and Agri-Food Canada, <https://sis.agr.gc.ca/cansis/nsdb/slc/v2.2>, 1996.
- 615 CLRTAP: Mapping critical loads for ecosystems, Chapter V of Manual on methodologies and criteria for modelling and mapping  
616 critical loads and levels and air pollution effects, risks and trends. UNECE Convention on Long-range Transboundary Air  
617 Pollution; accessed 09/16/2021 at [www.icpmapping.org](http://www.icpmapping.org), 2015.
- 618 Cronan, C. S. and Schofield, C. L.: Relationships between aqueous aluminum and acidic deposition in forested watersheds of  
619 North America and northern Europe, *Environ. Sci. Technol.*, 24, 1100–1105, <https://doi.org/10.1021/es00077a022>, 1990.
- 620 De Vries, W., Hettelingh, J.-P., and Posch, M. (Eds.): The History and Current State of Critical Loads and Dynamic Modelling  
621 Assessments, in: Critical loads and dynamic risk assessments: Nitrogen, acidity and metals in terrestrial and aquatic ecosystems,  
622 Springer, 1–11, 2015.





- 623 Dymond, C. C., Titus, B. D., Stinson, G., and Kurz, W. A.: Future quantities and spatial distribution of harvesting residue and  
624 dead wood from natural disturbances in Canada, *For. Ecol. Manag.*, 260, 181–192, <https://doi.org/10.1016/j.foreco.2010.04.015>,  
625 2010.
- 626 ECCC: Evaluation of the Addressing Air Pollution Horizontal Initiative, Environment and Climate Change Canada, ISBN: 978-  
627 0-660-39645-3, 2021.
- 628 ECCC: 2022 Canadian Protected and Conserved Areas Database (CPCAD) User Manual, *Environ. Clim. Change Can.*,  
629 [https://data-donnees.ec.gc.ca/data/species/protectstore/canadian-protected-conserved-areas-](https://data-donnees.ec.gc.ca/data/species/protectstore/canadian-protected-conserved-areas-database/ProtectedConservedAreaUserManual.pdf)  
630 [database/ProtectedConservedAreaUserManual.pdf](https://data-donnees.ec.gc.ca/data/species/protectstore/canadian-protected-conserved-areas-database/ProtectedConservedAreaUserManual.pdf), 2023a.
- 631 ECCC: Canadian Protected and Conserved Areas Database 2022 [dataset], Environment and Climate Change Canada,  
632 <https://www.canada.ca/en/environment-climate-change/services/national-wildlife-areas/protected-conserved-areas-database.html>,  
633 2023b.
- 634 ECCC: Toward a 2030 Biodiversity Strategy for Canada: Halting and reversing nature loss, Environment and Climate Change  
635 Canada, ISBN: 978-0-660-48594-2, 2023c.
- 636 ECCC: Canada's air pollutant emissions inventory report 1990-2022., Environment and Climate Change Canada. ISSN: 2562-  
637 4903. [https://publications.gc.ca/collections/collection\\_2024/eccc/En81-30-2022-eng.pdf](https://publications.gc.ca/collections/collection_2024/eccc/En81-30-2022-eng.pdf), Gatineau, Quebec, 2024.
- 638 FAO-UNESCO: Digital soil map of the world and derived soil properties, CD-ROM. Rome: FAO., 2003.
- 639 Feng, J., Vet, R., Cole, A., Zhang, L., Cheng, I., O'Brien, J., and Macdonald, A.-M.: Inorganic chemical components in  
640 precipitation in the eastern U.S. and Eastern Canada during 1989–2016: Temporal and regional trends of wet concentration and  
641 wet deposition from the NADP and CAPMoN measurements, *Atmos. Environ.*, 254, 118367,  
642 <https://doi.org/10.1016/j.atmosenv.2021.118367>, 2021.
- 643 Forsius, M., Posch, M., Aherne, J., Reinds, G., Christensen, J., and Hole, L.: Assessing the Impacts of Long-Range Sulfur and  
644 Nitrogen Deposition on Arctic and Sub-Arctic Ecosystems, *Ambio*, 39, 136–47, <https://doi.org/10.1007/s13280-010-0022-7>,  
645 2010.
- 646 Galmarini, S., Makar, P., Clifton, O. E., Hogrefe, C., Bash, J. O., Bellasio, R., Bianconi, R., Bieser, J., Butler, T., Ducker, J.,  
647 Flemming, J., Hodzic, A., Holmes, C. D., Kioutsioukis, I., Kranenburg, R., Lupascu, A., Perez-Camanyo, J. L., Pleim, J., Ryu,  
648 Y.-H., San Jose, R., Schwede, D., Silva, S., and Wolke, R.: Technical note: AQMEII4 Activity 1: evaluation of wet and dry  
649 deposition schemes as an integral part of regional-scale air quality models, *Atmospheric Chem. Phys.*, 21, 15663–15697,  
650 <https://doi.org/10.5194/acp-21-15663-2021>, 2021.
- 651 Hazlett, P., Emilson, C., Lawrence, G., Fernandez, I., Ouimet, R., and Bailey, S.: Reversal of Forest Soil Acidification in the  
652 Northeastern United States and Eastern Canada: Site and Soil Factors Contributing to Recovery, *Soil Syst.*, 4, 54,  
653 <https://doi.org/10.3390/soilsystems4030054>, 2020.
- 654 Hengl, T.: SoilGrids250m 2017-03 Absolute depth to bedrock (in cm). [dataset], ISRIC - World Soil Inf.,  
655 <https://data.isric.org/geonetwork/srv/api/records/f36117ea-9be5-4afd-bb7d-7a3e77bf392a>, 2017.
- 656 Hengl, T.: Clay content in % (kg / kg) at 6 standard depths (0, 10, 30, 60, 100 and 200 cm) at 250 m resolution (v0.2). [dataset],  
657 Zenodo, <https://doi.org/10.5281/zenodo.2525663>, 2018a.
- 658 Hengl, T.: Coarse fragments % (volumetric) at 6 standard depths (0, 10, 30, 60, 100 and 200 cm) at 250 m resolution [dataset],  
659 <https://doi.org/10.5281/zenodo.2525682>, 2018b.
- 660 Hengl, T.: Sand content in % (kg / kg) at 6 standard depths (0, 10, 30, 60, 100 and 200 cm) at 250 m resolution (v0.2) [dataset],  
661 Zenodo, <https://doi.org/10.5281/zenodo.2525662>, 2018c.
- 662 Hengl, T.: Soil bulk density (fine earth) 10 x kg / m-cubic at 6 standard depths (0, 10, 30, 60, 100 and 200 cm) at 250 m  
663 resolution (v0.2) [dataset], Zenodo, <https://doi.org/10.5281/zenodo.2525665>, 2018d.
- 664 Hengl, T. and Wheeler, I.: Soil organic carbon content in x 5 g / kg at 6 standard depths (0, 10, 30, 60, 100 and 200 cm) at 250 m  
665 resolution (v0.2) [dataset], Zenodo, <https://doi.org/10.5281/zenodo.2525553>, 2018.



- 666 Koseva, I. S., Watmough, S. A., and Aherne, J.: Estimating base cation weathering rates in Canadian forest soils using a simple  
667 texture-based model, *Biogeochemistry*, 101, 183–196, <https://doi.org/10.1007/s10533-010-9506-6>, 2010.
- 668 Lawrence, G. B., David, M. B., Lovett, G. M., Murdoch, P. S., Burns, D. A., Stoddard, J. L., Baldigo, B. P., Porter, J. H., and  
669 Thompson, A. W.: Soil Calcium Status and the Response of Stream Chemistry to Changing Acidic Deposition Rates, *Ecol.*  
670 *Appl.*, 9, 1059–1072, [https://doi.org/10.1890/1051-0761\(1999\)009\[1059:SCSATR\]2.0.CO;2](https://doi.org/10.1890/1051-0761(1999)009[1059:SCSATR]2.0.CO;2), 1999.
- 671 Lawrence, G. B., Hazlett, P. W., Fernandez, I. J., Ouimet, R., Bailey, S. W., Shortle, W. C., Smith, K. T., and Antidormi, M. R.:  
672 Declining Acidic Deposition Begins Reversal of Forest-Soil Acidification in the Northeastern U.S. and Eastern Canada, *Environ.*  
673 *Sci. Technol.*, 49, 13103–13111, <https://doi.org/10.1021/acs.est.5b02904>, 2015.
- 674 Li, H. and McNulty, S. G.: Uncertainty analysis on simple mass balance model to calculate critical loads for soil acidity, *Environ.*  
675 *Pollut.*, 149, 315–26, <https://doi.org/10.1016/j.envpol.2007.05.014>, 2007.
- 676 Liang, T. and Aherne, J.: Critical loads of acidity and exceedances for 1138 lakes and ponds in the Canadian Arctic, *Sci. Total*  
677 *Environ.*, 652, 1424–1434, <https://doi.org/10.1016/j.scitotenv.2018.10.330>, 2019.
- 678 Likens, G. E., Driscoll, C. T., and Buso, D. C.: Long-term effects of acid rain: response and recovery of a forest ecosystem,  
679 *Science*, 272, 244–246, <https://doi.org/10.1126/science.272.5259.244>, 1996.
- 680 Makar, P. A., Akingunola, A., Aherne, J., Cole, A. S., Aklilu, Y., Zhang, J., Wong, I., Hayden, K., Li, S.-M., Kirk, J., Scott, K.,  
681 Moran, M. D., Robichaud, A., Cathcart, H., Baratzedah, P., Pabla, B., Cheung, P., Zheng, Q., and Jeffries, D. S.: Estimates of  
682 exceedances of critical loads for acidifying deposition in Alberta and Saskatchewan, *Atmospheric Chem. Phys.*, 18, 9897–9927,  
683 <https://doi.org/10.5194/acp-18-9897-2018>, 2018.
- 684 McDonnell, T. C., Phelan, J., Talhelm, A. F., Cosby, B. J., Driscoll, C. T., Sullivan, T. J., and Greaver, T.: Protection of forest  
685 ecosystems in the eastern United States from elevated atmospheric deposition of sulfur and nitrogen: A comparison of steady-  
686 state and dynamic model results, *Environ. Pollut.*, 318, 120887, <https://doi.org/10.1016/j.envpol.2022.120887>, 2023.
- 687 McKenney, D., Papadopol, P., Campbell, K., Lawrence, K., Hutchinson, M., and others: Spatial models of Canada-and North  
688 America-wide 1971/2000 minimum and maximum temperature, total precipitation and derived bioclimatic variables. *Frontline*  
689 *Technical Note 106.*, 2006.
- 690 Mongeon, A., Aherne, J., and Watmough, S. A.: Steady-state critical loads of acidity for forest soils in the Georgia Basin, *British*  
691 *Columbia, J. Limnol.*, 69, 193–200, <https://doi.org/10.4081/jlimnol.2010.s1.193>, 2010.
- 692 Moran, M. D., Savic-Jovcic, V., Makar, P. A., Gong, W., Stroud, C. A., Zhang, J., Zheng, Q., Chen, J., Akingunola, A., Lupu, A.,  
693 Ménard, S., Menelaou, K., and Munoz-Alpizar, R.: Operational chemical weather forecasting with the ECCC online Regional Air  
694 Quality Deterministic Prediction System version 023 (RAQDPS023) - Part 1: System description, *Geosci Model Dev Prep.*,  
695 2024a.
- 696 Moran, M. D., Lupu, A., Savic-Jovcic, V., Zhang, J., Zheng, Q., Boutzis, E., Mashayekhi, R., Stroud, C. A., Ménard, S., Chen, J.,  
697 Menelaou, K., Munoz-Alpizar, R., Kornic, D., and Manseau, P.: Operational chemical weather forecasting with the ECCC online  
698 Regional Air Quality Deterministic Prediction System version 023 (RAQDPS023) - Part 2: Prospective and retrospective  
699 performance evaluations, *Geosci Model Dev Prep.*, 2024b.
- 700 Murray, C. A., Whitfield, C. J., and Watmough, S. A.: Uncertainty-based terrestrial critical loads of nutrient nitrogen in northern  
701 Saskatchewan, Canada, 22, 14, 2017.
- 702 NADP: National Trends Network [dataset], National Atmospheric Deposition Program (NRSP-3). NADP Program Office,  
703 Wisconsin State Laboratory of Hygiene, 465 Henry Mall, Madison, WI 53706, <https://nadp.slh.wisc.edu/networks/national-trends-network>, 2023.
- 705 NEG-ECP: Critical Load of Sulphur and Nitrogen Assessment and Mapping Protocol for Upland Forests, N. Engl. Gov. East.  
706 Can. Prem. Environ. Task Group Acid Rain Action Plan Halifax N. S., 2001.
- 707 Nilsson, J. and Grenfelt, P.: Critical levels for sulphur and nitrogen, 418 pp, Nord. Counc Minist Cph. Den., 1988.



- 708 Ouimet, R., Duchesne, L., Houle, D., and Arp, P.: Critical Loads and Exceedances of Acid Deposition and Associated Forest  
709 Growth in the Northern Hardwood and Boreal Coniferous Forests in Québec, Canada, *Water Air Soil Pollut. Focus*, 1, 119–134,  
710 <https://doi.org/10.1023/A:1011544325004>, 2001.
- 711 Ouimet, R., Arp, P. A., Watmough, S. A., Aherne, J., and DeMerchant, I.: Determination and Mapping Critical Loads of Acidity  
712 and Exceedances for Upland Forest Soils in Eastern Canada, *Water Air Soil Pollut.*, 172, 57–66, <https://doi.org/10.1007/s11270-005-9050-5>, 2006.
- 714 Pardo, L. H., Duarte, N., Miller, E. K., and Robin-Abbott, M.: Tree chemistry database (version 1.0), USDA For. Serv.  
715 Northeast. Res. Stn., 324, <https://doi.org/10.2737/NE-GTR-324>, 2005.
- 716 Pardo, L. H., Coombs, J. A., Robin-Abbott, M. J., Pontius, J. H., and D'Amato, A. W.: Tree species at risk from nitrogen  
717 deposition in the northeastern United States: A geospatial analysis of effects of multiple stressors using exceedance of critical  
718 loads, *For. Ecol. Manag.*, 454, 117528, <https://doi.org/10.1016/j.foreco.2019.117528>, 2019.
- 719 Paré, D., Bernier, P., Lafleur, B., Titus, B. D., Thiffault, E., Maynard, D. G., and Guo, X.: Estimating stand-scale biomass,  
720 nutrient contents, and associated uncertainties for tree species of Canadian forests, *Can. J. For. Res.*, 43, 599–608,  
721 <https://doi.org/10.1139/cjfr-2012-0454>, 2013.
- 722 Park, S. H., Gong, S. L., Gong, W., Makar, P. A., Moran, M. D., Zhang, J., and Stroud, C. A.: Relative impact of windblown dust  
723 versus anthropogenic fugitive dust in PM<sub>2.5</sub> on air quality in North America, *J. Geophys. Res. Atmospheres*, 115,  
724 <https://doi.org/10.1029/2009JD013144>, 2010.
- 725 Posch, M., de Smet, P. A. M., Hettelingh, J.-P., and Downing, R. J.: Calculation and Mapping of Critical Thresholds in Europe:  
726 Status Report 1999, Coordination Center for Effects, National Institute of Public Health and the Environment, Bilthoven,  
727 Netherlands, 1999.
- 728 Posch, M., de Vries, W., and Sverdrup, H. U.: Mass Balance Models to Derive Critical Loads of Nitrogen and Acidity for  
729 Terrestrial and Aquatic Ecosystems, in: *Critical Loads and Dynamic Risk Assessments: Nitrogen, Acidity and Metals in  
730 Terrestrial and Aquatic Ecosystems*, edited by: de Vries, W., Hettelingh, J.-P., and Posch, M., Springer Netherlands, Dordrecht,  
731 171–205, [https://doi.org/10.1007/978-94-017-9508-1\\_6](https://doi.org/10.1007/978-94-017-9508-1_6), 2015.
- 732 Pribyl, D. W.: A critical review of the conventional SOC to SOM conversion factor, *Geoderma*, 156, 75–83,  
733 <https://doi.org/10.1016/j.geoderma.2010.02.003>, 2010.
- 734 QGIS Development Team: QGIS Geographic Information System, QGIS Association, 2023.
- 735 Radke, L., Hegg, D., Lyons, J., Brock, C., Hobbs, P., Weiss, R., and Rasmussen, R.: Airborne measurements on smokes from  
736 biomass burning, *Aerosols Clim.*, 411–422, 1988.
- 737 Radke, L. F., Lyons, J. H., Hobbs, P. V., Hegg, D. A., Sandberg, D. V., and Ward, D. E.: Airborne monitoring and smoke  
738 characterization of prescribed fires on forest lands in western Washington and Oregon, US Department of Agriculture, Forest  
739 Service, Pacific Northwest Research Station, 1990.
- 740 Reinds, G. J., Posch, M., Aherne, J., and Forsius, M.: Assessment of Critical Loads of Sulphur and Nitrogen and Their  
741 Exceedances for Terrestrial Ecosystems in the Northern Hemisphere, in: *Critical loads and dynamic risk assessments: Nitrogen,  
742 acidity and metals in terrestrial and aquatic ecosystems*, edited by: De Vries, W., Hettelingh, J.-P., and Posch, M., Springer, 403–  
743 418, 2015.
- 744 Reinds, G. J., Thomas, D., Posch, M., and Slootweg, J.: Critical loads for eutrophication and acidification for European terrestrial  
745 ecosystems, Umweltbundesamt, Wörlitzer Platz 1, 06844 Dessau-Roßlau, Germany, 2021.
- 746 Rosen, K., Gundersen, P., Tegnhammar, L., Johansson, M., and Frogner, T.: Nitrogen enrichment of Nordic forest ecosystems:  
747 the concept of critical loads, *Ambio*, 21:5, 364–368, 1992.
- 748 Shangguan, W., Hengl, T., Mendes de Jesus, J., Yuan, H., and Dai, Y.: Mapping the global depth to bedrock for land surface  
749 modeling, *J. Adv. Model. Earth Syst.*, 9, 65–88, <https://doi.org/10.1002/2016MS000686>, 2017.
- 750 Simkin, S. M., Allen, E. B., Bowman, W. D., Clark, C. M., Belnap, J., Brooks, M. L., Cade, B. S., Collins, S. L., Geiser, L. H.,  
751 Gilliam, F. S., Jovan, S. E., Pardo, L. H., Schulz, B. K., Stevens, C. J., Suding, K. N., Throop, H. L., and Waller, D. M.:



- 752 Conditional vulnerability of plant diversity to atmospheric nitrogen deposition across the United States, *Proc. Natl. Acad. Sci.*,  
753 113, 4086–4091, <https://doi.org/10.1073/pnas.1515241113>, 2016.
- 754 Skeffington, R., Whitehead, P., and Abbott, J.: Quantifying uncertainty in critical loads: (B) Acidity mass balance critical loads  
755 on a sensitive site, *Water, Air, Soil Pollut.*, 169, 25–46, 2006.
- 756 SLCWG: Soil landscapes of Canada version 3.2 [dataset], Soil Landscapes of Canada Working Group. Agriculture and Agri-  
757 Food Canada, <https://sis.agr.gc.ca/cansis/nsdb/slc/v3.2/index.html>, 2010.
- 758 Statistics Canada: Agricultural ecumene boundary file, 2016 Census of Agriculture [dataset], Statistics Canada, Cat. No 92-639-  
759 X, <https://www150.statcan.gc.ca/>, 2017.
- 760 Sverdrup, H. and De Vries, W.: Calculating critical loads for acidity with the simple mass balance method, *Water, Air, Soil*  
761 *Pollut.*, 72, 143–162, <https://doi.org/10.1007/BF01257121>, 1994.
- 762 Sverdrup, H. and Warfvinge, P.: The effect of soil acidification effect on the growth of trees, grass and herbs, as expressed by the  
763 (Ca+ Mg+ K)/AL ratio, Reports in ecology and environmental engineering, Lund University Department of Chemical  
764 Engineering II, 1993.
- 765 Tegen, I. and Fung, I.: Contribution to the atmospheric mineral aerosol load from land surface modification, *J. Geophys. Res.*  
766 *Atmospheres*, 100, 18707–18726, <https://doi.org/10.1029/95JD02051>, 1995.
- 767 Tol, P.: Colour schemes, SRON Technical Note, Doc. no. SRON/EPS/TN/09-002, [https://personal.sron.nl/pault/colourschemes.](https://personal.sron.nl/pault/colourschemes.pdf)  
768 pdf, 2012.
- 769 Vandinther, N. and Aherne, J.: Biodiversity-Based Empirical Critical Loads of Nitrogen Deposition in the Athabasca Oil Sands  
770 Region, *Nitrogen*, 4, 169–193, <https://doi.org/10.3390/nitrogen4020012>, 2023a.
- 771 Vandinther, N. and Aherne, J.: Ecological Risks from Atmospheric Deposition of Nitrogen and Sulphur in Jack Pine forests of  
772 Northwestern Canada, *Nitrogen*, 4, 102–124, <https://doi.org/10.3390/nitrogen4010008>, 2023b.
- 773 de Vries, W., Posch, M., Reinds, G. J., and Kämäri, J.: Critical loads and their exceedance on forest soils in Europe, Report - The  
774 Winand Staring Centre for Integrated Land, Soil and Water Research (SC\_DLO), Wageningen, the Netherlands, 123 pp., 1992.
- 775 Whitfield, C. J., Aherne, J., Watmough, S. A., and McDONALD, M.: Estimating the sensitivity of forest soils to acid deposition  
776 in the Athabasca Oil Sands Region, Alberta, *J. Limnol.*, 69, 201, <https://doi.org/10.4081/jlimnol.2010.s1.201>, 2010.
- 777 Wilkins, K., Cathcart, H., Hickey, P., Hanley, O., Vintró, L. L., and Aherne, J.: Influence of Precipitation on the Spatial  
778 Distribution of 210Pb, 7Be, 40K and 137Cs in Moss, *Pollutants*, 3, 102–113, <https://doi.org/10.3390/pollutants3010009>, 2023.
- 779 Williston, P., Aherne, J., Watmough, S., Marmorek, D., Hall, A., de la Cueva Bueno, P., Murray, C., Henolson, A., and  
780 Laurence, J. A.: Critical levels and loads and the regulation of industrial emissions in northwest British Columbia, Canada,  
781 *Atmos. Environ.*, 146, 311–323, <https://doi.org/10.1016/j.atmosenv.2016.08.058>, 2016.
- 782 Wu, W. and Driscoll, C. T.: Impact of Climate Change on Three-Dimensional Dynamic Critical Load Functions, *Environ. Sci.*  
783 *Technol.*, 44, 720–726, <https://doi.org/10.1021/es900890t>, 2010.
- 784 Zhao, W., Zhao, Y., Ma, M., Chang, M., and Duan, L.: Long-term variability in base cation, sulfur and nitrogen deposition and  
785 critical load exceedance of terrestrial ecosystems in China, *Environ. Pollut.*, 289, 117974,  
786 <https://doi.org/10.1016/j.envpol.2021.117974>, 2021.

787